SIMULATION FOR PREDICTION OF LAND SUBSIDENCE DUE TO GROUNDWATER WITHDRAWAL IN BANGKOK AREA, THAILAND

PEE POATPROMMANEE

MASTER OF SCIENCE
IN GEOLOGY

GRADUATE SCHOOL
CHIANG MAI UNIVERSITY
MAY 2019

SIMULATION FOR PREDICTION OF LAND SUBSIDENCE DUE TO GROUNDWATER WITHDRAWAL IN BANGKOK AREA, THAILAND

PEE POATPROMMANEE

A THESIS SUBMITTED TO CHIANG MAI UNIVERSITY IN PARTIAL FULFILLMENT OF THE REQUIREMENTS FOR THE DEGREE OF MASTER OF SCIENCE IN GEOLOGY

GRADUATE SCHOOL, CHIANG MAI UNIVERSITY
MAY 2019

SIMULATION FOR PREDICTION OF LAND SUBSIDENCE DUE TO GROUNDWATER WITHDRAWAL IN BANGKOK AREA, THAILAND

PEE POATPROMMANEE

THIS THESIS HAS BEEN APPROVED TO BE A PARTIAL FULFILLMENT
OF THE REQUIREMENTS FOR THE DEGREE OF
MASTER OF SCIENCE
IN GEOLOGY

Examination Committee:

.... Chairman
(Dr. Phayom Saraphirom)

.... Member
(Asst. Prof. Dr. Kannipa Motanated)

.... Member
(Asst. Prof. Dr. Schradh Saenton)

Advisor:

....
(Asst. Prof. Dr. Schradh Saenton)

17 May 2019

ACKNOWLEGEMENT

This study would not be completed without the support from many people. I gratefully thank Asst. Prof. Dr. Schradh Saenton, my advisor. He supports me in every part of recharge from beginning to end. He gives support and comments when I face the difficult times. His comment makes this study better. I thank the Department of Groundwater Resource (DGR) that has kindly supplied information about the lower Chao Phraya aquifer system for this study. I also thank Dr. Phayom Saraphirom and Asst. Prof. Dr. Kannipa Motanated for their comments in the final version of thesis.

Finally, I thank my family, my friends, faculty members and staffs and other people who give help and support me in many things throughout my study period and cheer me up in the difficult times

Pee Poatprommanee

หัวข้อวิทยานิพนธ์	การจำลองเพื่อทำนายการทรุดตัวของแผ่นดินเนื่องจากการสูบน้ำบาดาลในเขตพื้นที่กรุงเทพมหานคร ประเทศไทย
ผู้เขียน	นายพีร์ พจน์พรหมมณี
ปริญญา	วิทยาศาสตรมหาบัณฑิต (ธรณีวิทยา)
อาจารย์ที่ปรึกษา	ผู้ช่วยศาสตราจารย์ ดร. จิรัฏฐ์ แสนทน

บทคัดย่อ

กรุงเทพมหานครตั้งอยู่ในพื้นที่ราบน้ำท่วมถึงของแม่น้ำเจ้าพระยา ซึ่งเป็นพื้นที่ค่อนข้างราบและสม่ำเสมอ มีความสูงเฉลี่ยประมาณ 1.5 เมตรจากระดับน้ำทะเล ระบบน้ำบาดาลในแอ่งเจ้าพระยาประกอบด้วยชั้นกรวด ทรายแทรกสลับกับชั้นดินเหนียว ชั้นตะกอนเหล่านี้ถูกแบ่งเป็น ชั้นดินเหนียวและชั้นน้ำบาดาลจำนวน 8 ชั้นได้แก่ ชั้นน้ำบาดาลกรุงเทพฯ ชั้นน้ำบาดาลพระประแดง ชั้นน้ำบาดาลนครหลวง ชั้นน้ำบาดาลนนทบุรี ชั้นน้ำบาดาลสามโคก ชั้นน้ำบาดาลพญาไท ชั้นน้ำบาดาลธนบุรี และชั้นน้ำปากน้ำ โดยมีบันทึกการเริ่มใช้น้ำบาดาลตั้งแต่ช่วงประมาณ พ.ศ. 2440 และอัตราการสูบน้ำมีการเพิ่มขึ้นอย่างต่อเนื่อง จนกระทั่งในปี พ.ศ. 2523 ปริมาณการใช้น้ำบาดาลสูงกว่า 1.2 ล้านลูกบาศก์เมตรต่อวัน หลังจากนั้น อัตราการใช้น้ำค่อนข้างคงที่และลดลงเล็กน้อย เนื่องจากมีการประกาศมาตรการควบคุมการใช้น้ำบาดาล ซึ่งการใช้น้ำบาดาลในปริมาณมากเป็นเวลานานจากชั้นน้ำบาดาลกรุงเทพฯ ชั้นน้ำบาดาลพระประแดง ชั้นน้ำบาดาลนครหลวง ชั้นน้ำบาดาลนนทบุรี ส่งผลให้เกิดการทรุดตัวของแผ่นดินที่สามารถสังเกตได้ทั่วไป โดยในปี พ.ศ. 2524 อัตราการทรุดตัวถูงถึง 120 มิลลิเมตรต่อปี และลดลงเป็น 20 มิลิเมตรต่อปี ในปี พ.ศ. 2545 พบว่ามีการทรุดตัวสะสมในเขตตัวเมืองประมาณ 1.60 เมตร ในช่วงปี พ.ศ. 2476-2530 และเพิ่มเป็น 2.05 เมตรในปี พ.ศ. 2545

การศึกษาครั้งนี้ ได้ทำการจำลองการไหลของน้ำบาดาลและการทรุดตัวของแผ่นดินโดยใช้โปรแกรม MODFLOW ซึ่งพื้นที่ศึกษามีขนาดประมาณ 70×80 ตารางกิโลเมตร ครอบคลุมพื้นที่ในเจ็ดจังหวัดได้แก่ กรุงเทพมหานคร ปทุมธานี นนทบุรี นครปฐม สมุทรสาคร สมุทรปราการ และพระนครศรีอยุธยา ระบบน้ำบาดาลได้ถูกแบ่งออกเป็นกริดจำนวน 40 แถวและ 35 หลัก โดยแต่ละกริดมีขนาด 2×2 ตารางกิโลเมตร และทำการจำลองชั้นหินอุ้มน้ำจำนวน 5 ชั้น ซึ่งแบ่งเป็นชั้นดินเหนียว

และชั้นน้ำบาดาลหลักจำนวน 4 ชั้นบนสุดที่มีการใช้น้ำ โดยทำการจำลองการไหลในภาวะคงตัวและไม่คงตัว ตั้งแต่ พ.ศ. 2553-2559 และปรับเทียบแบบจำลองโดยใช้ข้อมูลระดับน้ำจากบ่อสังเกตการณ์จำนวน 66 แห่งโดยโปรแกรมปรับเทียบจำลองแบบอัตโนมัติ (PEST) ร่วมกันกับการประยุกต์ใช้จุดนำร่อง (pilot points) แบบจำลองการไหลของน้ำบาดาลที่ถูกปรับเทียบแล้วจะนำมาใช้ในการจำลองการทรุดตัวของแผ่นดินในช่วงเวลาเดียวกัน โดยใช้ข้อมูลการทรุดตัวจาก 37 ตำแหน่งวัดมาใช้ในการปรับเทียบแบบจำลองให้สอดคล้องกับสภาพการทรุดตัวของพื้นที่ จากนั้นจึงนำแบบจำลองที่ได้ไปใช้ทำนายสถานการณ์การทรุดตัวในอีก 20 ปีข้างหน้า

ผลการศึกษาการจำลองการไหลของน้ำบาดาลพบว่าอัตราการสูบน้ำที่ควรจะเป็น มีค่าประมาณ 1.5 เท่าของปริมาณการใช้น้ำบาดาลทั้งหมดที่รายงานจากบ่อที่ขึ้นทะเบียน และชั้นน้ำบาดาลชั้น 1 แสดงพฤติกรรมเป็นชั้นน้ำบาดาลแบบไม่มีแรงดัน ส่วนชั้นน้ำบาดาลชั้นที่ 3 4 และ 5 แสดงพฤติกรรมของชั้นน้ำบาดาลแบบมีแรงดัน และส่วนชั้นน้ำบาดาลชั้นที่สองแสดงพฤติกรรมทั้งสองแบบ การทำนายระดับของน้ำบาดาลในอนาคตแสดงให้เห็นว่าระดับน้ำบาดาลในหลาย ๆ พื้นที่มีการเพิ่มสูงขึ้นเนื่องจากมีการใช้น้ำน้อยลง ยกเว้นบริเวณที่เป็นกรวยน้ำลดเดิม จะมีระดับน้ำบาดาลลดต่ำลงมากขึ้น ผลการจำลองการทรุดตัวของแผ่นดินพบว่า พื้นที่ส่วนใหญ่สามารถจำลองการทรุดตัวของแผ่นดินได้และผลการจำลองสอดคล้องกับข้อมูลที่ได้จากการบันทึกในภาคสนาม ยกเว้นบริเวณขอบทางทิศใต้ซึ่งใกล้กับขอบเขตที่เป็นอ่าวไทย ผลการจำลองยังพบอีกว่า พื้นที่ส่วนใหญ่มีการทรุดตัวสะสมลดลง โดยบริเวณที่มีการทรุดตัวสะสมสูงสุดอยู่ในจังหวัดปทุมธานีซึ่งมีการทรุดตัว 6.5 เซนติเมตร และบริเวณที่มีการคืนตัวสะสมสูงสุดอยู่ในเขตกรุงเทพมหานคร โดยมีการคืนตัวประมาณ 8 เซนติเมตร

Thesis Title Simulation for Prediction of Land Subsidence Due to Groundwater Withdrawal in Bangkok Area, Thailand

Author Mr. Pee Poatprommanee

Degree Master of Science (Geology)

Advisor Asst. Prof. Dr. Schradh Saenton

ABSTRACT

Bangkok is located in the Chao Praya river floodplain. This area is flat and low-lying landscape with an average elevation of about 1.5 m above mean sea level. The Bangkok aquifer system consisted of multiple layers of interbedded clay and aquifer layers. Major aquifers of the Chao Praya basin can be divided into top clay layer and 8 major aquifers consisting of Bangkok (or BK), Phra Pradaeng (PD), Nakorn Luang (or NL), Nonthaburi (NB), Sam Khok (SK), Phaya Thai (PT), Thonburi (TB), and Paknam (or PK) from top to bottom. Groundwater extraction in Bangkok aquifer system was officially recorded and dated back to early 1900s. The amount of groundwater pumping continuously increased. The pumping rate increased to 1.2 million m^3/d in 1980. After which, an extraction rate was stable and slightly decreased due to groundwater usage control policy. However, the pumping rate increased again to 2.2 million m^3/d in 2000. The largest amount of groundwater has been extracted from PD, NL, and NB aquifers. The long-term use of groundwater caused land subsidence that can be observed throughout the whole Bangkok and metropolitan areas. The land subsidence rate was as high as 120 mm/yr in 1981 and dropped to 20 mm/yr in 2002 but the area of land subsidence had expanded. The largest cumulative land subsidence in the city area was 1.60 m during a period of 1933-1987 and increased to 2.05 m in 2002.

This study aimed to setup groundwater flow and land subsidence model based on MODFLOW program. The study area covers the area of 70×80 km^2 from seven provinces including Bangkok, Pathum Tani, Nonthaburi, Nakhonpathom, Samut Sakhon, Samut

Prakan, and Phra Nakorn Si Ayutthaya. The model domain was divided into 35 columns, 40 rows where each grid size is 2×2 km^2 grid size, and five layers including top clay layer and four additional layers of main aquifers. The steady-state and transient groundwater flow model was simulated from January 2010 to June 2016. The flow model was calibrated systematically and automatically using parameter estimation code (PEST) based on hydraulic heads measured from 66 observation wells as calibration targets. The “pilot point” technique was used to calibrate for model parameters such as hydraulic conductivity, storage coefficient, specific yield, recharge and evapotranspiration. The calibrated groundwater flow model was subsequently used to setup land subsidence model using inter-bed storage (IBS) package. The subsidence model was calibrated based on subsidence data monitored at 37 locations. The model was then used to predict flow and subsidence scenario for the next 20 years.

The results indicated that the flow model can successfully simulate steady-state and transient conditions. It was found that groundwater usage or pumping rates should have been approximately 1.5 times larger than the reported groundwater usage from registered wells. It was also found that layer 1 (from top) is unconfined whereas model layer 3, 4, and 5 are confined. Layer 2, however, showed both confined and unconfined behaviors. The predicted model showed that groundwater level, in general, tended to increase but the existing cones of depression. The calibrated land subsidence model was able to capture subsidence phenomena acceptably well although subsidence in southern boundary, near Gulf of Thailand, did not give acceptable results. Subsidence prediction showed that cumulative land subsidence tended to stabilize with time. The maximum cumulative land subsidence was 6.5 cm in Pathum Thani and maximum surface rebound was 8.0 cm in Bangkok.

CONTENTS

LIST OF TABLES

LIST OF FIGURES

CHAPTER 1

INTRODUCTION

1.1 Background and problems

Groundwater extraction in the Bangkok metropolitan and nearby areas have been officially documented since mid-1900s due to the lack of surface water supply and groundwater was an alternative and reliable water resource for public water supply (IGES, 2007). The amount of groundwater usage was continuously increased and peaked during late 1970s and early 1980s, and slowly declined after implementation of control measures in 1983 (Figure 1.1). However, insufficient public water supply system in suburban areas has caused an increase in exploitation of groundwater especially from private wells. The private wells are the major groundwater consumers in Bangkok metropolitan and its vicinities. The excessive groundwater extraction has led to the lowering of pore water pressure in aquifer as well as the clay layers and seams. While the groundwater head drops in the clay structure, the consolidation process starts and results in land subsidence will be resulted. Land subsidence has been a continuing problem in Bangkok for the past four decades. In 1969, land subsidence was given widespread attention when the several significant subsidence was observed in Bangkok area (AIT, 1982). The groundwater withdrawal caused approximately 0.5 m of land subsidence in Central Bangkok in 1978 (AIT, 1981).

Recently, there has been a lower groundwater extraction rate which leads to the decreasing rate of land subsidence. The Department of Groundwater Resource (DGR) has monitored and collected relevant data related to land subsidence such as the distribution of vertical displacements, the groundwater level and the groundwater usage in Bangkok and vicinity provinces since 2000s. However, the compiled data have not been analyzed nor numerically simulated and verified. The numerical model can be used to the quantitatively predict land subsidence. Thus, this research aims at developing a numerical model for simulating land subsidence due to groundwater withdrawal based on the new dataset compiled by DGR. The study area is located in the lower Chao Phraya basin and covers the areas of seven provinces that include Bangkok, Pathum Tani, Nonthaburi, Nakhonpathom, Samut Sakhon, Samut Prakan, and Phra Nakorn Si Ayutthaya. The study area is located in latitude 13°27′25.6″ N to 14°10′34.4″ N and longitude 100°11′30.2″ E to 100°50′38.0″ E (Figure 1.2). The model will be calibrated and verified using subsidence dataset and subsequently used to predict future land subsidence that may take place.

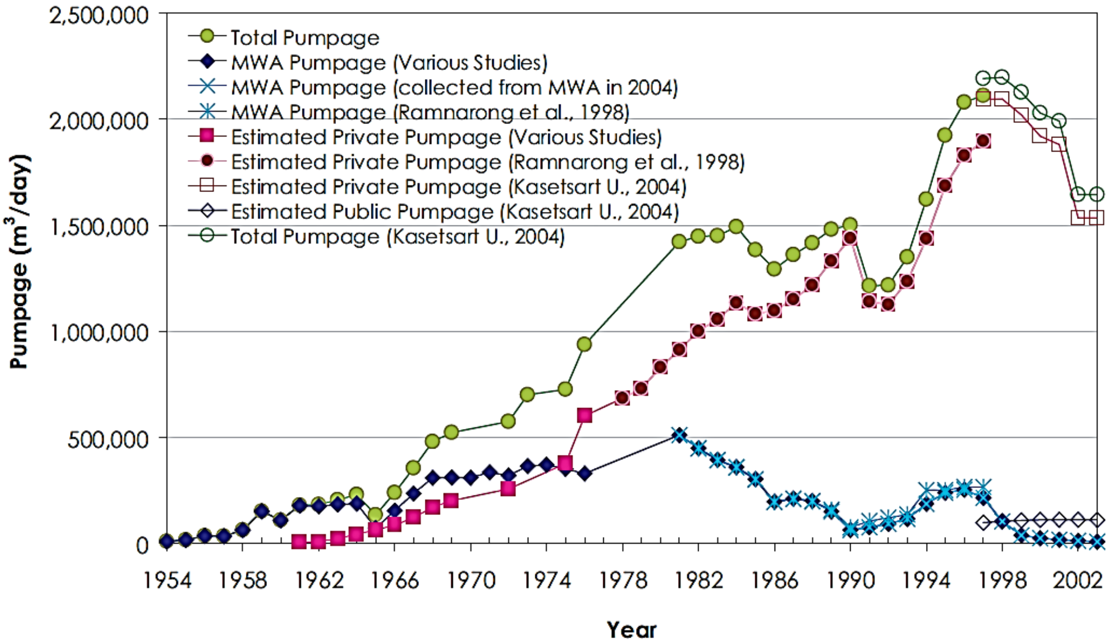

Figure 1.1 Groundwater pumping in Bangkok and vicinity areas (IGES, 2007).

1.2 Objective and scopes

1.2.1 Objective

1) To develop a calibrated and verified numerical groundwater flow model of Bangkok aquifer system.

2) To simulate and predict previous and ongoing land subsidence in Bangkok and vicinity areas.

1.2.2 Scope

This research focuses on understanding aquifer system response to groundwater withdrawal and land subsidence behavior in the lower Chao Phraya basin. The groundwater modelling technique is used to stimulate stead-state and transient groundwater flow model based on finite-difference method. The measured groundwater heads were used as observation data for model calibration. The calibrated groundwater flow model will subsequently be used to simulate land subsidence. It is expected that the land subsidence model can be practically used for groundwater resource planning and prediction of future land subsidence.

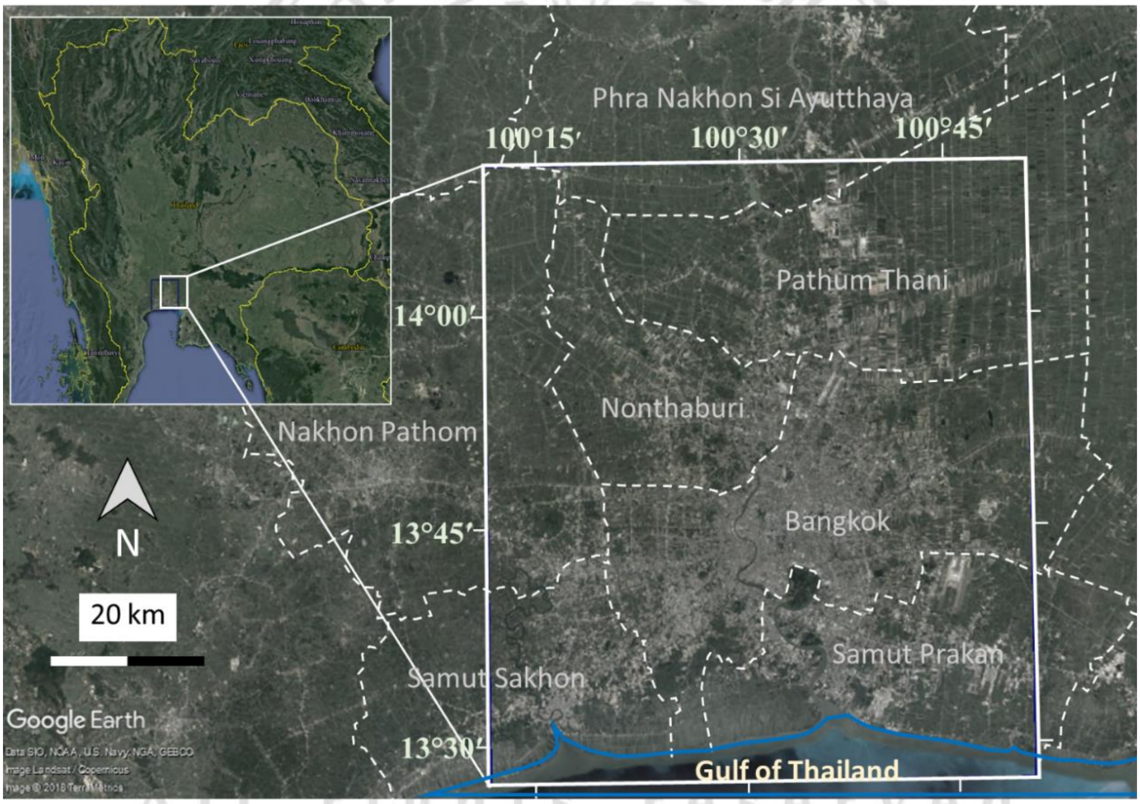

Figure 1.2 Study area (modified from Google Earth®).

1.3 Overview of research methodology

The model for groundwater flow and land subsidence simulation will be constructed, executed and calibrated. A numerical model setup was initiated by constructing a conceptual model representing a system that is made of a set concepts to understand or model the real system. The conceptual model of this research is constructed using surface elevation, hydrogeological cross-sections and land use maps. The finite difference groundwater flow model, MODFLOW (Harbaugh *et al.*, 2000; Harbaugh, 2005), is converted from the conceptual model, aquifer properties from pumping test data, groundwater pumping rate, recharge from water balance, evapotranspiration, and necessary boundary conditions. The model is executed under steady-state and transient conditions. An inverse modeling code, PEST (Doherty, 1994), which is the automatic calibration algorithm is used for sensitivity analysis and to perform model calibration. The calibrated groundwater flow model is subsequently used for simulation of land subsidence based on Inter-Bed Storage (IBS) package of MODFLOW program (Leake and Prudic, 1991). The IBS package requires additional model input data on elastic and inelastic coefficients. Measured land subsidence data is used to calibrate subsidence model.

CHAPTER 2

LITHERATURE REVIEW

2.1 General information of study area

2.1.1 Topography

Bangkok and vicinity areas are located in the Chao Praya river floodplain whose setting is in the lower part of central Thailand. The area is flat and low-lying landscape with an elevation ranging approximately from 0 to 5 m above mean sea level (~1.5 m amsl. in average). The basin is filled with the flood plain and delta sediments and marine deposits as a result of the change in sea level during the Quaternary period (Likitlersuang *et al.*, 2013). The Chao Praya river meanders through the middle of study area to Gulf of Thailand in Samut Prakan (Figure 2.1). Tha Chin river is distributary of Chao Phraya river that separates in Chai Nat and flows parallel to the main river and discharges to the Gulf of Thailand in Samut Sakhon which is about 35 kilometers in westward of Chao Phraya river estuary.

2.1.2 Climate

Central Thailand is located in tropical zone with 2 seasons that are wet and dry. The dry season is in the period of October to April (about 7-8 months). During this phase there is almost no precipitation. The wet season starts in May and ends in October (about 4-5 months) and more than 80 percent of annual precipitation takes place during this period. The average of annual rainfall in Bangkok from 2003 to 2015 is approximately 1600 mm and raining session is about 127 days (NSO, 2016).

2.1.3 Hydrology, geology and hydrogeology

The basement structure of the lower Chao Phraya basin is still not clearly understood. The Chao Phraya Basement which is a complex metamorphic and plutonic rock was dropped into graben by block faulting (primary fault in North-South direction) in Late Pliocene-Pleistocene (Nutalaya and Rau 1987). In Tertiary and Quaternary period, the basin was filled with a sequence of unconsolidated clastic sediments that consist of alluvial sand and gravel interbedded with floodplain silt and clay grading to marine clay. The unconsolidated sediments beneath the lower part of the Central Thailand plain can be divided to 8 aquifers (Figure 2.2). However, the leakage of the clay layers is estimated over the large area since the unconnected aquitard may have large discontinuities therefore the groundwater withdrawal in one aquifer may lower hydraulic head (i.e., groundwater potentiometric surface) to the entire aquifer system.

Figure 2.1 Chao Phraya river drainage (modified from Wikipedia).

The uppermost aquifer is Bangkok (BK) aquifer is located at the depth of ~50 m with average thickness of 20 to 30 m. The groundwater in Bangkok aquifer may generally not be consumable due to its high salinity and partly contamination from borrow pit excavation for landfill material that used to fill the surface level of construction sites (Phien-wej *et al.*, 2006). The Bangkok aquifer is separated by the interbedded hard clay layers. The depth of upper Bangkok aquifer is 16 to 30 m and the lower Bangkok aquifer is 35 to 55 m. They are also known as the first and second sand layer in foundation engineering.

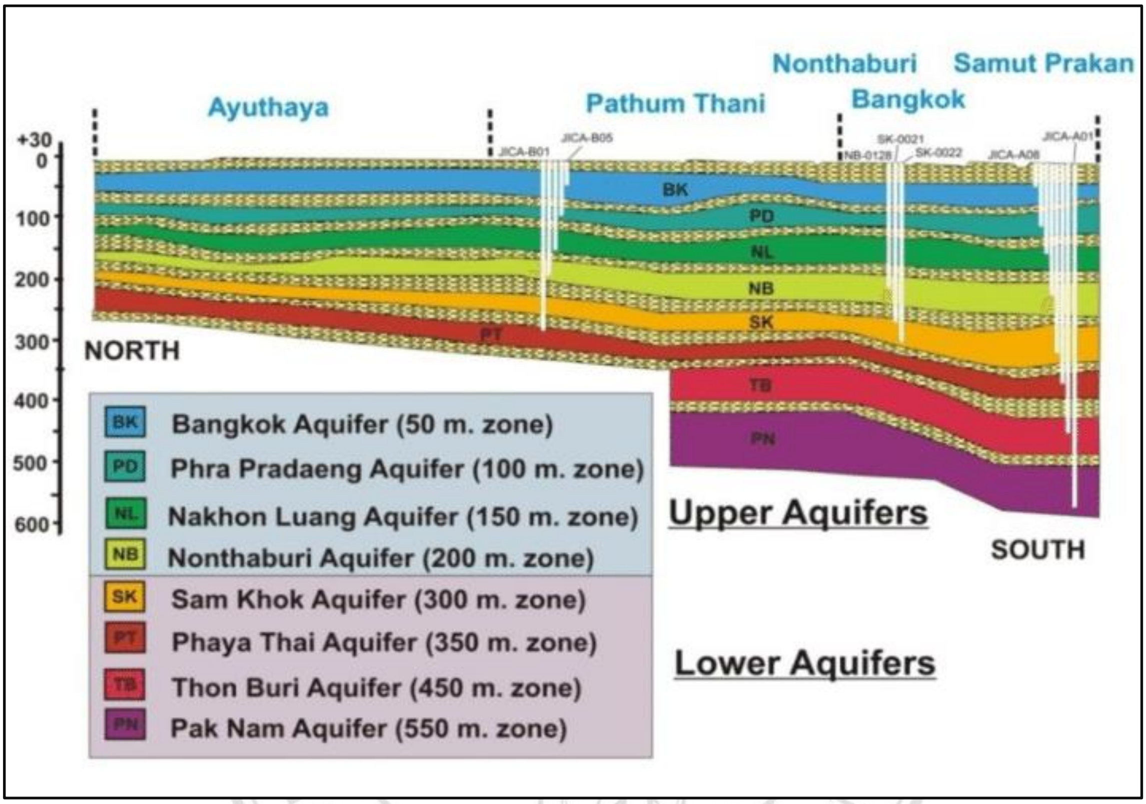

Figure 2.2 Section of Bangkok aquifer system from North to South in Central Thailand plain (Noipow et al., 2016).

The second, third and fourth aquifers are highly productive aquifers namely the Phra Pradaeng (PD) aquifer of 100 m deep and the Nakorn Luang (NL) aquifer of 150 m deep and the Nonthaburi (NB) aquifer of 200 m deep (Ramnarong *et al.*, 1998). The highest pumping rate occurred in NL aquifer which accounts for approximately 50% of total extraction. Groundwater of PD aquifer is widely used in most areas except in the southern part of Bangkok where water quality is saline and cannot be used. The groundwater quality in NL aquifer is generally good except in the northwest and southwest areas of Bangkok where the groundwater is brine. The pumping wells in the two mostly used aquifers (NL and NB aquifers) were reported to groundwater yield at rate of 100 to 300 m^3/hr. Deep groundwater extraction in some areas had become necessary in 1990s-2000s because of the drastic drop in groundwater level causing sea water intrusion in these aquifers (Phien-wej *et al.*, 2006 and Ramnarong *et al.*, 1998). The

Sam Khok (SK) aquifer, located at 300 m deep, and the Phaya Thai (PT) aquifer, 350 m deep, are currently not in use due to their greater depth and lower yield. Groundwater of the Thonburi (TB) aquifer, 450 m deep, and Paknam (PK) aquifer, 550 m deep, have been proved to be the source of fresh water but have been tapped by only few deep wells (Nguyen, 1999; Rotchanameka and Mairaing 2013).

2.1.4 Groundwater usage and land subsidence

In early 1900s, the deep groundwater extraction in Bangkok aquifer system was started, then in the early 1950s, the extraction rate had increased to the large quantity (Ramnarong *et al.*, 1998). Figure 2.3 shows groundwater extraction rates in Bangkok and surrounding provinces during 1960s to 2000s. In 1975, the pumping rate was recorded at about 0.65 Mm^3/d and rapidly increased to 1.2 Mm^3/d in 1980. The Royal Thai Government initiated a project called “The Migration of Groundwater Crisis and Land Subsidence in Bangkok Metropolis”. The resolution of the issue confirmed that high rate of groundwater extraction was the cause of land subsidence. Several measures were released to control and reduce groundwater extraction which was the reason for stabilized and slightly decreased groundwater pumping rate during a period of mid 1980s to 1990s. The pumping rate was greatly decreased in the inner-city area where the public water supply was available. However, after 1993 the groundwater extraction rate rapidly increased due to a new wave of economic growth. After that, the city rapidly expanded to the suburbs where water supply was not sufficient. Consequently, groundwater has inevitably been used to supply the developmental process in this area. In 2000, it was reported that groundwater was extracted up to 2.2 Mm^3/d by the registered pumping well (Phien-wej *et al.*, 2006)

The over groundwater pumping during 1970s-1980s had led to a strong and wide range drawdown that covered the entire metropolis area. In NL and NB aquifers, the piezometric head dropped up to 40 to 50 m. The cone of depression center was observed in the eastern district where was the center of residential and industrial growths. During 1990s, the continuous increase in groundwater pumping rate induced further significant drawdown. Figure 2.4 presents a contour map of groundwater level (or potentiometric surface head) from the NL aquifer in 2002 and thee largest depression cone occurred in eastern part of the metropolitan area. The lowest piezometric surface of the cone was 65 m below the ground level which was 15-m lower than that measured in 1981. The size of the main cone had expanded following the city growth. The smaller size drawdown cone occurred in the industrial suburban area, southwest Bangkok, where lacked the surface water supply (Phien-wej *et al.*, 2006).

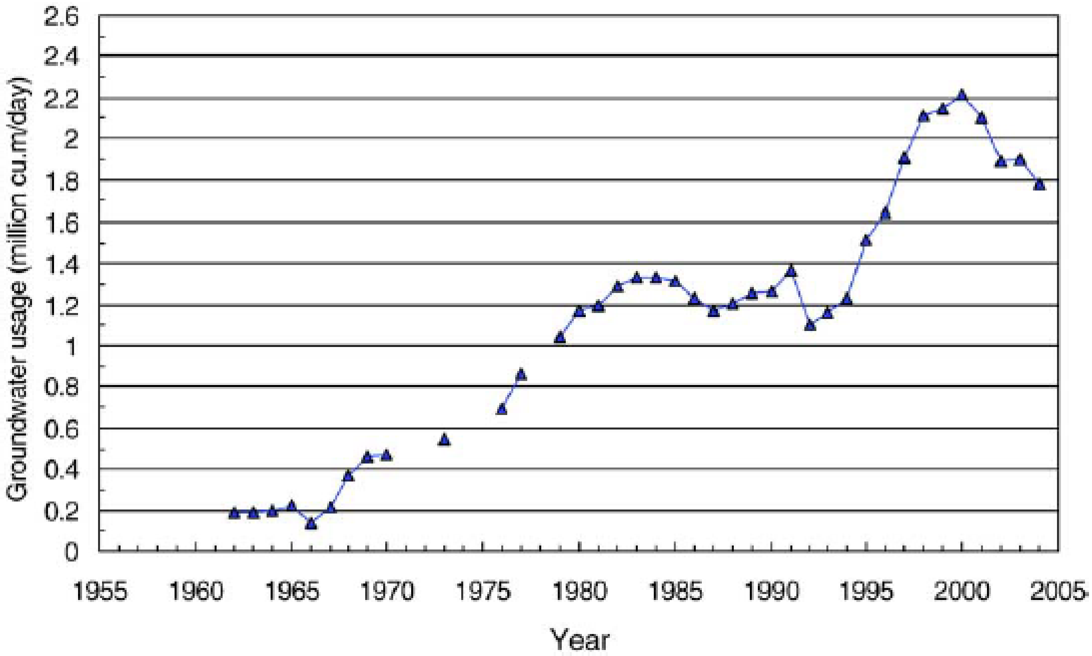

Figure 2.3 Groundwater usage in Bangkok plain during 1955-2004 (after Phien-wej *et al.*, 2006).

The report of land subsidence in Bangkok was initially documented by Cox (1968). According to AIT (1981), the main cause of land subsidence was the excessive groundwater extraction. The evidence of land subsidence can be observed ubiquitously throughout the whole city in form of the separation and settlement of footpath and ground from adjoining buildings, buckling pavement over footing, and differential subsidence between building. (Figure 2.5). Nutalaya *et al.* (1989) reported the largest land subsidence in the city area of 1.60 m over 54-year period from 1933 to 1987. Subsequent data showed land subsidence increased to 2.05 in 2002 (Phien-wej *et al.*, 2006). Figure 2.6 shows the comparison of subsidence rates between 2002 and 1981 as shown in Figure 2.6a and Figure 2.6b, respectively). Although the subsidence rate had decreased significantly, it expanded to the vicinity areas. In 1981, the subsidence rate in Bangkok area was as high as 120 mm/yr but decreased slowly to 20 mm/yr in 2002. At the same time, the maximum subsidence rate of 30 mm/yr occurred in southeast and southwest districts where heavy industries developed. The inner part of the Bangkok area where the heavy groundwater pumping had started since 1970s, the land subsidence rate ranged from 5 to 10 mm/yr as a result of transient consolidation behavior of surface soft clay layer. The groundwater level had not been recovered since the increased groundwater extraction in 1980s. The land subsidence in this area had been continuously occurring in small rate over the past decades (AIT 1981 and Phien-wej *et al.*, 2006)

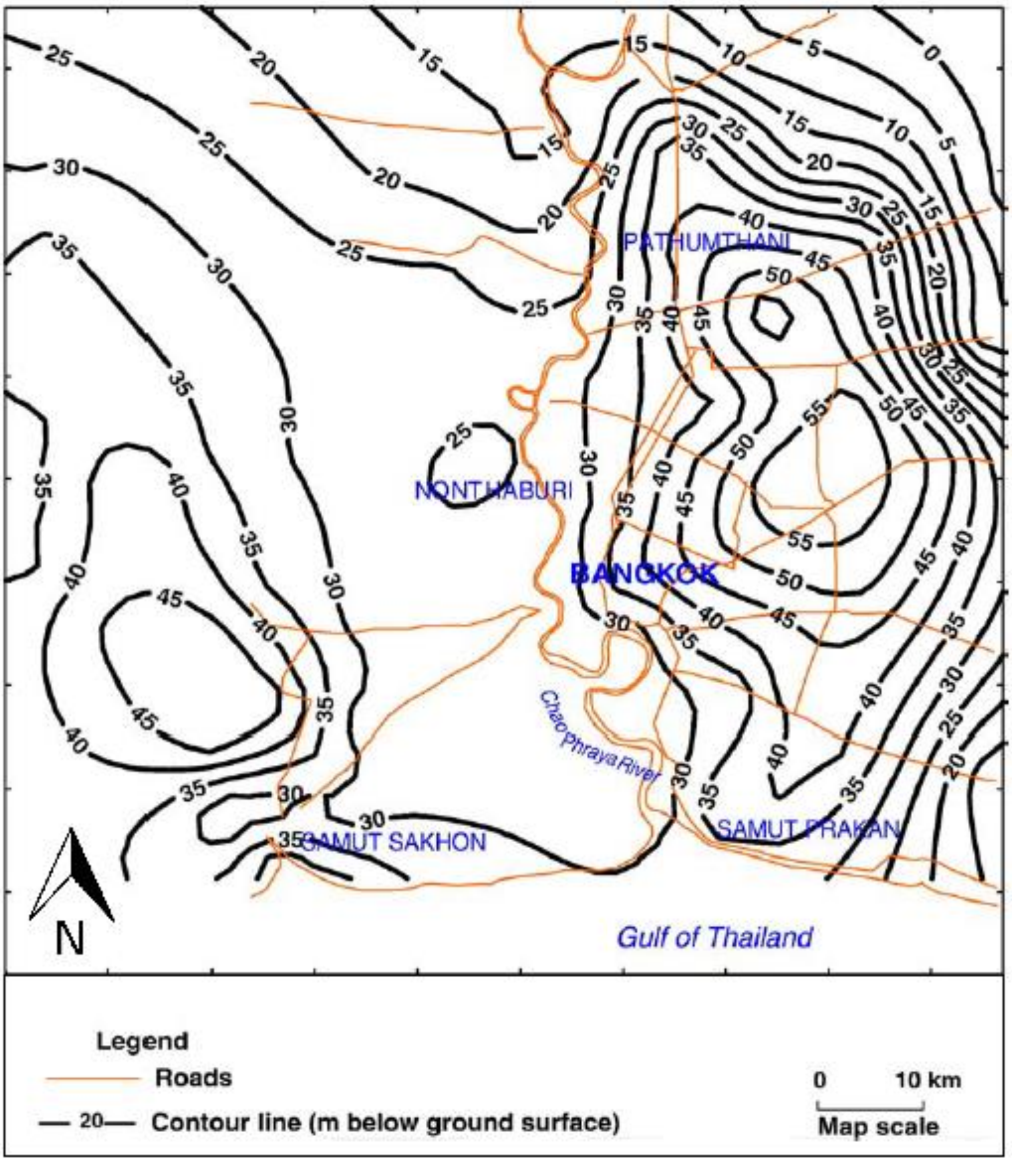

Figure 2.4 Piezometric head from NL aquifer in 2002 (Phien-wej *et al*., 2006).

Figure 2.5 Land subsidence damage to building (after Phien-wej *et al.,* 2006 and 1998).

In recent years, land subsidence has been systematically monitored and documented by Department of Groundwater Resources or DGR (2018) in “The Study of Effect on Groundwater System in Groundwater Critical Zone and Lower Chao Phraya Basin Project”. In the third progress report, the situation of land subsidence was mentioned as follows.

During 1978 to 1982, eastern Bangkok had an average land subsidence rate of 9 cm/yr with the maximum rate of 10 cm/yr whereas in western Bangkok land subsidence was gentle at an average rate 0.9 cm/yr. The northern Bangkok, average land subsidence occurred at a rate of 5.5 cm/yr where in central area subsidence rate was 4.1 cm/yr. In metropolitan area such as Nonthaburi, land subsidence rate was reported to be 4.6 cm/yr.

critical zones consisted of four provinces including Bangkok, Nonthaburi, Pathum Thani, and Samut Prakan. The regulation imposed a high groundwater usage fee of 1

THB/m^3 in 1985. The average land subsidence in eastern, western, and central Bangkok were 2, 0.1 and 0.8 cm/yr, respectively. The subsidence rates in the metropolitan areas such as Nonthaburi, Pathum Thani, Samut Prakan, Samut Sakhon and Nakhon Pathom were 1.4, 1.9, 4.6, 1.0 and 2.5 cm/yr, respectively

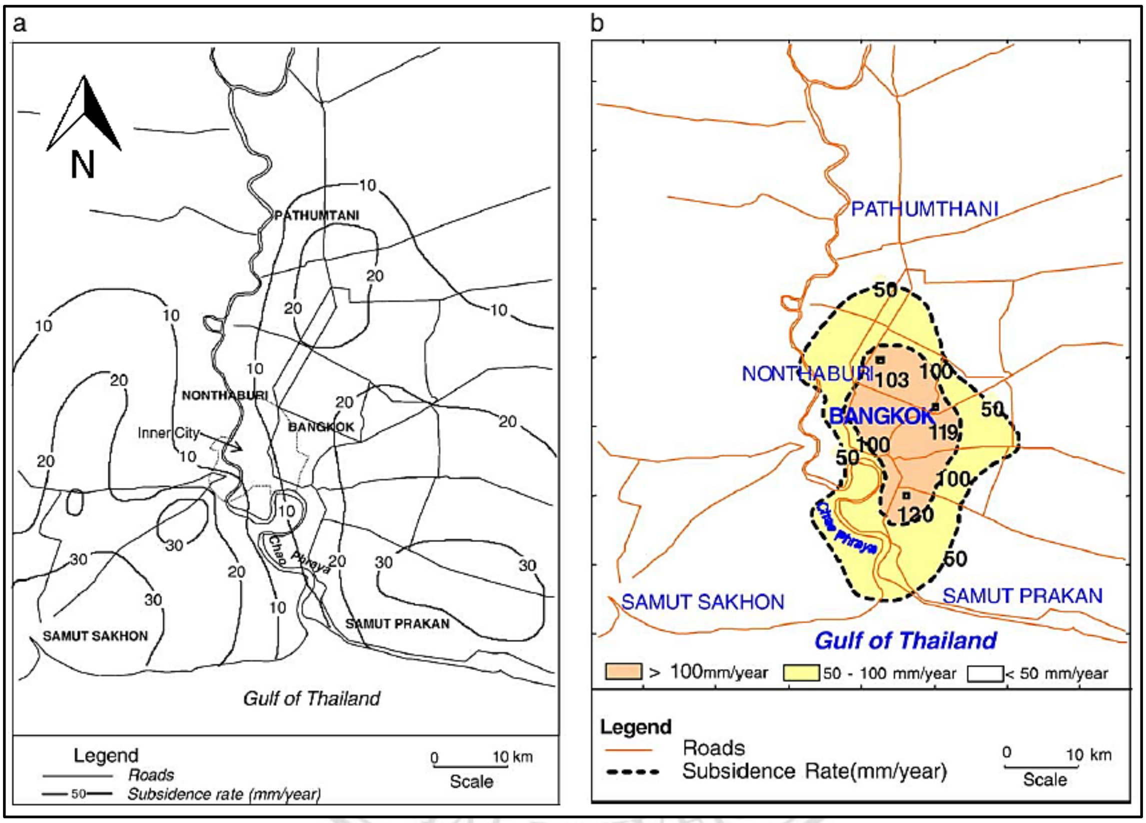

Figure 2.6 Land subsidence rate a: in 2002 and b: 1981 (after Phien-wej *et al.*, 2006 and AIT 1981).

In 1988 to 1992, average land subsidence in eastern, western, northern and central Bangkok were 2.2, 0.5, 1.9 and 1.0 cm/yr, respectively. In the metropolitan areas, the subsidence rates were 0.4, 0.5, 4.9, 2.2, and 2.6 cm/yr in Nonthaburi, Pathum Thani, Samut Prakan, Samut Sakhon, and Nakhon Pathom, respectively.

During 1993 to 1997, the second set of groundwater critical zones was announced. In this announcement, three additional provinces were added including Nakhon Pathom, Samut Sakhon, and Phra Nakhon Sri Ayutthaya. In addition, groundwater usage fee was increased to 3.5 THB/m^3 starting in 1994. Despite the aforementioned regulations, land subsidence still continuously occurred at the rates of 2.4, 0.4, 2.9 and 0.9 cm/yr in eastern, western, northern and central Bangkok, respectively. The land surface started to rebound at the rates of 0.4 and 0.9 cm/yr in Nonthaburi and Pathum Thani, respectively. In Samut Prakan, subsidence rate was 6.3 cm/yr. Land subsidence rated 2.5 cm/yr in Samut Sakhon and 2.0 cm/yr in Nakhon Pathom.

During 1998 to 2002, the third groundwater critical zone announcement was released in previously regulated seven provinces and groundwater usage fee increased to 8.5 THB/m^3 starting in 2000. As a result, eastern Bangkok had average subsidence rate of 0.4 cm/yr. There was a rebound in some areas of western Bangkok with 0.4 cm/yr rebound rate. In Nonthaburi and Pathum Thani provinces, ground surface rebounded with rate of 0.3 and 0.5, respectively. The average of subsidence rate was reported as 2.3 cm/yr in Samut Prakan, 2.0 cm/yr in Samut Sakhon, and 1.6 cm/yr in Nakhon Pathom.

During 2003 to 2005, new groundwater usage fee announcement was implemented under the new name, Groundwater Conservation Fee. Such fee imposed additional groundwater charge of 8.5 THB/m^3 which increased total fee to 17 THB/m^3 for groundwater users in the seven regulated provinces. There was still a continuous subsidence in Bangkok. The average subsidence rate in was 2.4 cm/yr eastern Bangkok, 1.5 cm/yr in western Bangkok and 2.4 cm/yr in central areas. Nonthaburi province had average subsidence rate of 1.3 cm/yr whereas Pathum Thani province had rebound with the rate of 2.4 cm/yr. Samut Prakan, Samut Sakhon and Nakhon Pathom had average subsidence rates of 2.0, 2.0 and 1.6 cm/yr.

In 2006, a "BMR 5" benchmark that was one of elevation reference points in Ratchaburi had subsided for 14 cm so land subsidence measurement was reset in this year. During 2006 to 2012, Bangkok metropolitan area had average smaller land subsidence rate in the range of 0 to 1 cm/yr Some areas had land subsidence in rate of 1 to 2 cm/yr where only few areas such as Mueang Samut Sakhon District had subsidence rate of 2 to 3 cm/yr.

In 2014, land subsidence magnitude was compared with re-calibrated elevation of benchmark which was established in 2012. Among 40 benchmarks, initially installed at 1-meter depth, 17 benchmarks subsided whereas the other 23 bench marks were elevated or raised. Almost all of subsidence magnitude was in range of 0 to 2 cm but Thanyaburi

District, Pathum Thani, subsided at a rate of 2.14 cm/yr. Almost all of 27 deeper (at depth greater than 1 m) benchmarks were elevated. Only few benchmarks subsided. However, such survey was conducted and launched during wet season when groundwater was probably recharged or replenished and, consequently, may cause the elevated benchmarks. In later years, the survey is often launch in dry season.

The study by Faculty of Engineering Chulalongkorn University (2009) on the "Analysis of Land Subsidence in Bangkok and its Vicinity Area" reported percentage of total land subsidence as a function of depth as shown in Table 2.1 and the cause(s) of subsidence in Table 2.2.

Table 2.1 Distribution of land subsidence from the past to 2007 varying with depths (modified after Faculty of Engineering Chulalongkorn University, 2009).

Station	Percent of total subsidence with depth (%)		
	0-50 m	>50 m	0-20m
8	89.60	10.40	54.38
20	71.15	28.85	22.12
30	79.80	20.20	69.18
32	66.63	33.37	3.96

Table 2.2 Percentage of land subsidence due to the causes (modified after Faculty of Engineering Chulalongkorn University, 2009).

Area	Causes			
	Building and land reclamation Load (%)	Groundwater extraction (%)	Natural Subsidence (%)	Subsidence rate (cm/yr)
Eastern Bangkok	50	50	negligible	-1.00
Western Bangkok	55	45	negligible	-1.10

Table 2.3 Percentage of land subsidence due to the causes (modified after Faculty of Engineering Chulalongkorn University, 2009). (continued)

Area	Causes			
	Building and land reclamation Load (%)	Groundwater extraction (%)	Natural Subsidence (%)	Subsidence rate (cm/yr)
Phra Nakhon Sri Ayutthaya	27	73	negligible	-0.0001
Nonthaburi	18	82	negligible	-1.20
Nakhon Pathom	2	98	negligible	-1.50
Samut Sakhon	24	70	6	-4.00
Pathum Thani	18	80	2	-0.10
Southern Samut Prakan	33	60	7	-2.10
Northern Samut Prakan	35	65	negligible	-1.70

2.2 Principle and theory of groundwater flow

2.2.1 Aquifer properties

There are several physical properties of rocks or sediments that control groundwater resource. However, the most important properties are storativity (or storage coefficient, S) and hydraulic conductivity (K) which are related to formation's porosity and permeability, respectively. Porosity is the ratio of void to bulk volume of material that can be used to imply the quantity of groundwater may be stored in material. However, some pores are disconnected to other pores causing the pore water in these pores non-extractable. The effective porosity refers to the interconnected pore. In the coarse geologic materials such as sand and gravel, the effective porosity is almost equal to overall porosity. In the finer sediments, effective porosity may be lower because the capillary force between water and material in small pore hinders water transmissivity.

Effective porosity is normally low in crystalline rock that does not have appreciable degree of fracture or weathering.

Hydraulic conductivity (which is related to the formation's permeability) is a property of rock or soil that transmit water. Hydraulic conductivity is affected by size, shape and interconnecting pore spaces (Driscoll, 1986). The unit of hydraulic conductivity is length per time (such as m/d or ft/d). Hydraulic conductivity values in rock and soil varies significantly. Non-fractured crystalline rock may have hydraulic conductivity ranging from the value of as low as 10^{-8} ft/d to as high as 10^{4} ft/d. In clay or clay-rich formation, hydraulic conductivity ranges from 10^{-7} to 10^{-3} ft/d (Heath, 1983). Anisotropy ratio is ratio of hydraulic conductivity in different directions. For example, anisotropy ratio of vertical permeability (K_v) to horizontal permeability (K_h) is given by K_v/K_h. Todd (1980) reported anisotropy ratio value ranging 0.1 to 0.5 for alluvium and may be lower to 0.01 when clay layer is presented.

2.2.2 Darcy's law and groundwater flow equation

The groundwater flow relates to potential energy that is described by hydraulic head. Hydraulic head is combination of water elevation (i.e., potential) and pressure. Groundwater moves response to the difference of hydraulic head from higher energy point to lower energy point. In a regional scale, this process makes groundwater flow from recharge to discharge areas. The groundwater flow rate depends on hydraulic conductivity and difference of hydraulic head over distant (which is called a hydraulic gradient). In mid-19th century, Henry Darcy derived an equation that describe water flow through porous medium with difference hydraulic head and distant (Figure 2.7). Darcy's law (Darcy, 1856):

$$Q = KA\frac{\Delta h}{\Delta l} \tag{2-1}$$

where Q is volume of water flow through porous medium, K is hydraulic conductivity of medium, A is cross-sectional area of medium, Δh is hydraulic head drop over a distance Δl. Darcy's law provides average volumetric flow rate of groundwater through porous media. Natural groundwater flow rate is generally slow and can be found in the range of 1-100 m/yr (Freeze and Cherry, 1979).

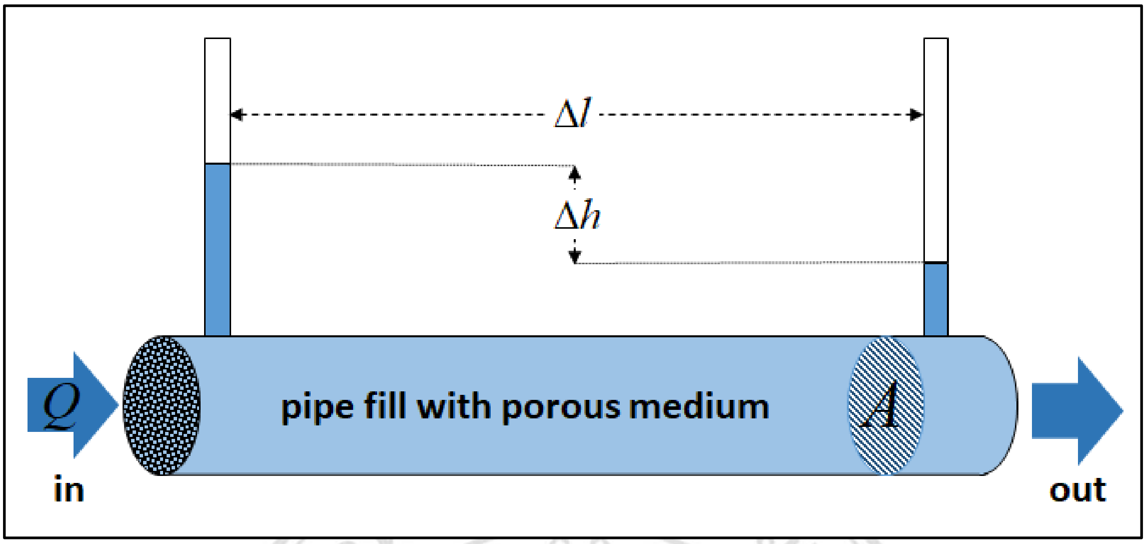

Figure 2.7 Darcy's experiment (modified after Darcy, 1856).

The numerical model, MODFLOW (Harbaugh *et al.*, 2000; Harbaugh, 2005), is a modular three-dimensional finite-difference groundwater model of the U.S. Geological Survey that can be used to simulate and predict the behavior of groundwater systems. The original version of MODFLOW (McDonald and Harbaugh, 1988) can simulate the effect of pumping wells, rivers, drains, head-dependent boundaries, recharge, and evapotranspiration. Since the publication of MODFLOW, various codes have been developed and they are called packages. The package is a specific feature of hydrologic system to be simulated. The models and programs communicate with MODFLOW through data files. MODFLOW combined conservation of mass and Darcy's law to simulate transient groundwater flow in aquifer systems based on the equation (2-2)

$$S_s \frac{\partial h}{\partial t} = K_x \frac{\partial^2 h}{\partial x^2} + K_y \frac{\partial^2 h}{\partial y^2} + K_z \frac{\partial^2 h}{\partial z^2} \pm W, \qquad (2\text{-}2)$$

where K_x, K_y, and K_z are hydraulic conductivities along the x, y, and z directions, respectively. The variable h is the hydraulic head, W refers to source/sink of groundwater (i.e., boundary conditions) which has a unit of T^{-1}, S_s is aquifer's specific storage, and t is time.

2.3 Land subsidence

2.3.1 Theory of land subsidence

Figure 2.8 shows subsidence process caused by lower groundwater level with long term groundwater extraction. When the groundwater pressure or head is lowered, the pore water pressure in sand and/or gravel layer quickly decrease but in clay layer the pore water pressure gradually decreases at a slower rate because of its low hydraulic conductivity. The excess pore water pressure will decrease with time and increases stress on clay structure beyond the preconsolidation pressure. So, the clay layer will undergo compaction and the land subsidence will occur.

Consolidation is any process that decreases pore water pressure from saturated soil without replacing water with air that decreases the volume of clay layer. The consolidation processes generally occur with groundwater withdrawal and long-term static load. Terzaghi (1943) derived the partial differential equation (equation (2-3)) to describe the consolidation processes in the horizontal beds of ideal saturated clay by

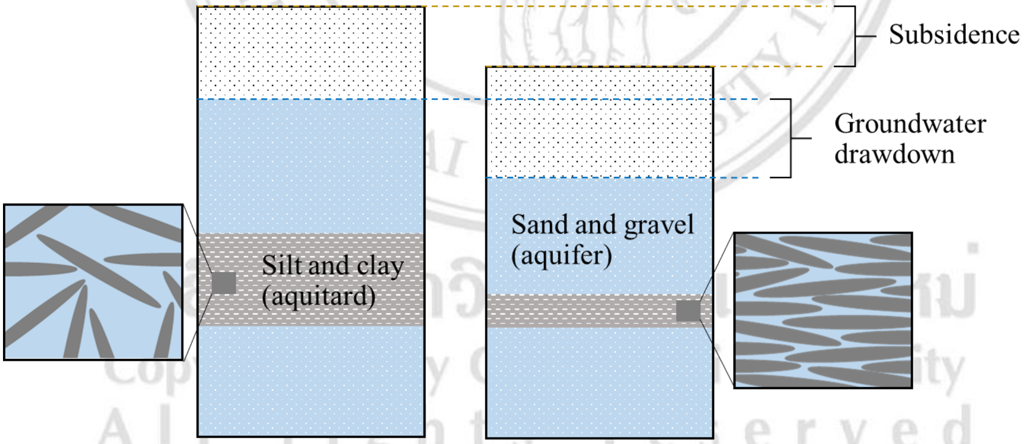

Figure 2.8 Mechanism of subsidence due to groundwater drawdown.

assuming that water and soil particles are perfectly incompressible, Darcy's law is strictly valid, hydraulic conductivity is constant, and the consolidation time lag due to the lower permeability of clay layer:

$$\frac{\partial u}{\partial t} = c_v \frac{\partial^2 u}{\partial z^2}, \qquad (2\text{-}3)$$

where u is excess hydraulic pressure, t is time, z is depth, and c_v is coefficient of consolidation. The parameter c_v (L^2/T) is used to describe the compression process. The rate and amount of compression in soils or aquifer materials varies with the rate of pore water pressure lost. The parameter c_v can be defined as the following:

$$c_v = \frac{K(1+e_\circ)}{\gamma_w}\left(-\frac{\Delta P}{\Delta e}\right), \tag{2-4}$$

where K is hydraulic conductivity, $e_\circ$ is initial void ratio, γ_w is unit weight of water, P is pressure and e is void ratio. The $\Delta e/\Delta P$ ratio is called coefficient of compressibility (a_v) that describes the change in void ratio when pressure changes. And, the ratio $a_v/(1+e_\circ)$ is the coefficient of volume decrease (m_v).

2.3.2 Land subsidence modeling

Land subsidence due to groundwater withdrawal can be simulated using Interbed Storage or IBS package (Leake and Prudic, 1991) in MODFLOW program (Harbaugh, 2005). The IBS package defines land subsidence based on the principle of effective stress. In confined aquifer, the change in effective stress depends on groundwater level as the following equation:

$$\Delta p' = -\gamma_w \Delta h, \tag{2-5}$$

where $\Delta p'$ is the change in effective stress (positive for increase and negative for decrease), γ_w is unit weight of water, and Δh is change in hydraulic head (positive for increase and negative for decrease). In an unconfined aquifer, the change in effective stress is smaller than confined aquifer because some moisture remains in unsaturated zone and $\Delta p'$ is defined as:

$$\Delta p' = -\gamma_w \Delta h(1-n+n_w), \tag{2-6}$$

where n is porosity and n_w is ratio of moisture or water content to total volume.

The relationship between elastic compaction (or expansion) of sediments change in effective stress is defined as:

$$\Delta b = \frac{\Delta p'}{\gamma_w} S_{ske} b_0 , \qquad (2\text{-}7)$$

where Δb is change in thickness (positive for compaction and negative for expansion), S_{ske} is the skeleton component of elastic storage coefficient, and b_0 is initial thickness of the interbedded seams or layers. The sediment compaction behavior is elastic until the effective stress is beyond the previous maximum stress. The compaction per unit in inelastic behavior is considerably greater than elastic behavior. The approximate inelastic compaction is:

$$\Delta b^* = \frac{\Delta p'}{\gamma_w} S_{skv} b_0 , \qquad (2\text{-}8)$$

where Δb^* is approximate inelastic compaction and S_{skv} is the skeleton component of inelastic storage coefficient. The IBS package in MODFLOW requires input of elastic and inelastic coefficients for every aquifer to compute compaction and subsidence.

CHAPTER 3

METHODOLOGY

3.1 Overview

This chapter describes the methods and techniques that are used to set up the groundwater flow model and land subsidence model of the lower central Thailand plain based on hydrogeological data. This study focuses on unconsolidated and semi-consolidated aquifers and aquitards. The numerical model of this study is constructed by the MODFLOW-2000 and MODFLOW-2005 that was developed by Harbaugh *et al.*, (2000) and Harbaugh (2005) respectively. The pilot-point model calibration approach is used to automatically and systematically calibrate heterogeneous aquifers model based on observation hydraulic head using PEST algorithm (Doherty, 1994 and Doherty, 2003). There are three main steps to set up the model. The first step is developing a conceptual model and transforming into a grid or numerical model. Then, steady-state and transient flow modeling are executed and calibrated. The last step is to apply the calibrated flow model to simulate (as well as calibrate) the land subsidence model. The calibrated flow and subsidence models will then be used in short- and long-term prediction.

3.1.1 Modeling guideline

Groundwater flow modeling normally follows steps and protocols suggested by Anderson and Woessener (1992). Figure 3.1 shows the workflow of the groundwater flow modeling steps which can be described below.

1. Modeling purpose identification: This step focuses on clearly identifying the objective(s) of the modeling. The purpose of model is the primary factor to be considered when selecting the appropriate method, model dimension (2D or 3D), and time (transient or steady-state), and in addition, the purpose leads to how the model is developed. The one of common purposes is to forecast the results (head and flow) of future action or condition, but models are also used to simulate past condition.

2. Model conceptualization: This step identifies and describes the model boundary, hydrological unit and the groundwater flow system that include storage and movement of groundwater in the aquifer system. This step includes assembling data on aquifer's hydraulic parameters.

3. Model design and construction: This step transforms conceptual model into mathematical or numerical model by defining the grid system, setting boundary conditions and stresses (e.g., pumping wells, recharge, evapotranspiration, rivers, etc.), and assigning (or assuming, if unknown or not measured) the aquifer parameters values, initial conditions and stress periods and time steps in transient model.

4. Model calibration: The calibration is considered to be the most important processes in groundwater modeling (Doherty, 1994). It involves the processes to estimate parameters describing groundwater system in order to simulate or match the model with the field observations, called history matching. History matching operation consists of sequence of modulating the initial parameters and running the model until the result of model is close to calibration targets. Calibration process can be achieved through manual or trial-and-error procedure and/or automated parameter estimated code that helps find the best possible parameters. The calibrated parameters are then used in model prediction. The simple model is easy to construct, simulate, and calibrate but it cannot match the history data. The complex model is usually better for history matching but it takes longer time to execute and calibrate. However, some of complexity is necessary to history matching but it should not be too complex. Thus, the balance between complexity and simplicity is important.

5. Model prediction: The goal of this step is to answer the specific questions from modeling objectives. The predictive model utilizes the calibrated model to forecast the responding of groundwater system in future conditions. The prediction model uses the final calibrated parameters except the parameters that are expected to change in the future.

6. Uncertainty analysis: Model uncertainty should be reported. The uncertainty in model occurs from model simplification, model calibration, parameter assumption, and time-dependent hydraulic condition. The uncertainty analysis includes error in measurement, model design error, and uncertainty in future hydraulic parameters. The uncertainty presentation should include a visual depiction that shows the model prediction is not only a result or a set of results.

7. Report and archiving: The model results are indicated in model report and gathered in model archive. The model report records the modelling processes and shows results, conclusions, and limitations. It includes information of the materials and the hydrogeologic setting, explanation of the data and assumption that are used to construct the conceptual model and a reference to the numerical method and code selection. The report is described how model domain is discretized and how parameters are assigned, associated calibration processes, and shown calibration results, prediction result, and uncertainty analysis. The modelling report should be accompanied by an archive of all model datasets and supporting files such as input and output file, so the results in the report are used to re-create the model in the future.

3.2 Data compilation

The conceptual model was constructed in the very first step of groundwater modeling protocol. The required data for setting up the groundwater flow model in the study area consisted of hydrological framework and hydrological stress. The hydrological framework describes the physical properties of system and parameter that does not vary with time. The hydrological stress describes the dynamic of groundwater system. All of the data was compiled and analyzed to establish the conceptual model

The three-dimension finite-difference groundwater flow model in this study was set up by using the data that consisted of surface elevation in the form of Digital Elevation Model (DEM), hydrogeological cross-sections, hydraulic properties of hydrological units, historical groundwater usage data, and groundwater level. The surface elevation data is acquired from Jarvis *et al*. (2008). The initial hydrologic properties (if unavailable) were approximated from JICA (1995). The other data was acquired from Department of Groundwater Resources (DGR). The observation wells are shown in Figure 3.2 and Table 3.2. For land subsidence model, the land subsidence data acquire from Chaithavee (2015) and DGR (2015).

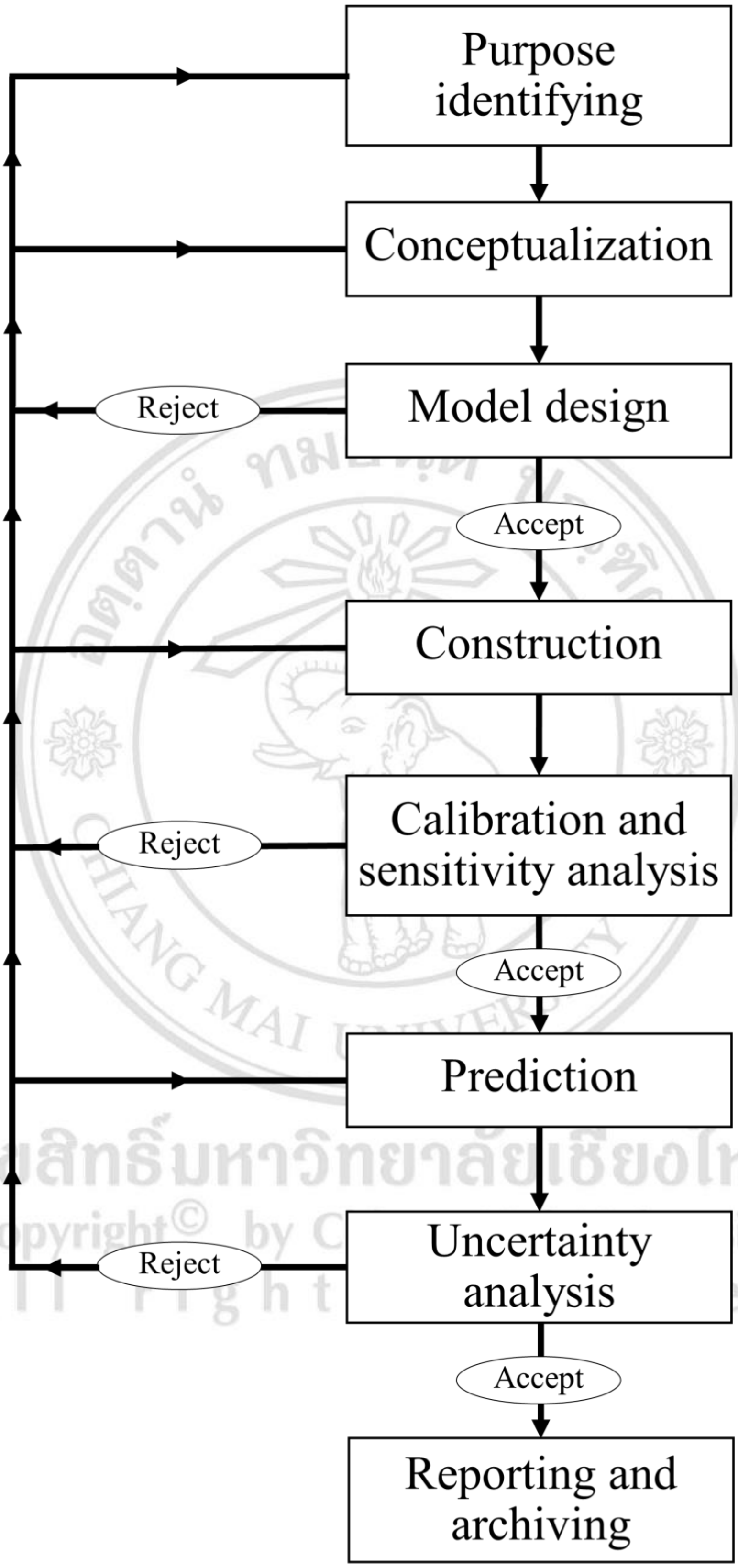

Figure 3.1 Workflow of groundwater flow model setup (modified from Anderson and Woessener, 1992).

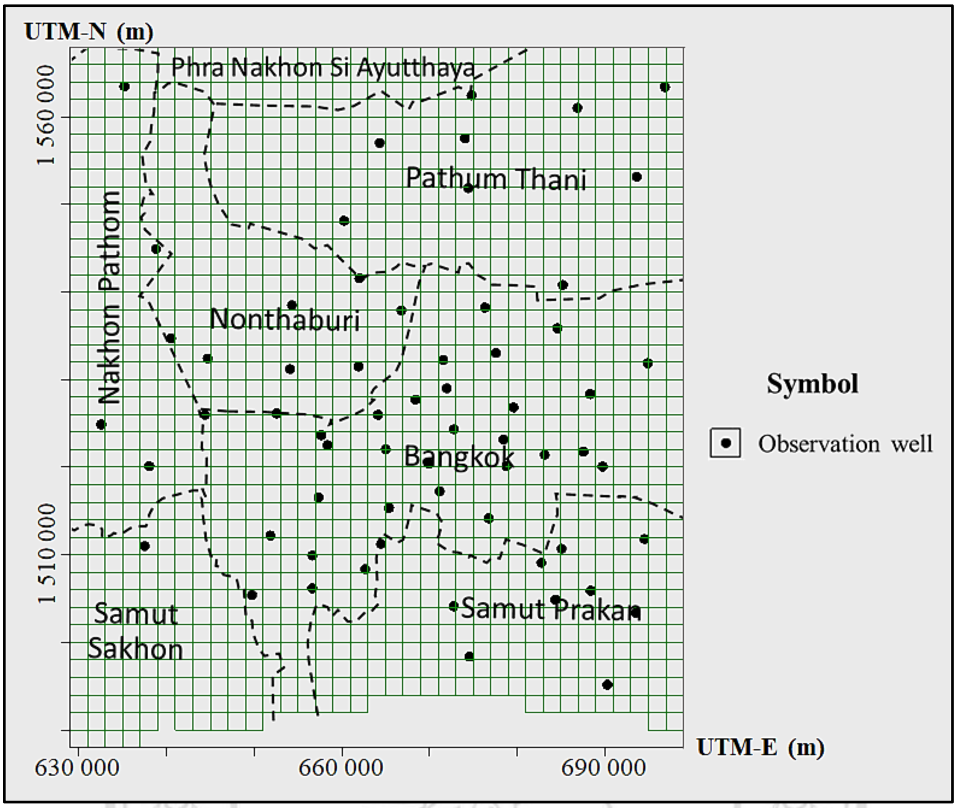

Figure 3.2 Observation well locations.

Table 3.1 Locations of groundwater monitoring wells.

Well NO.	UTM-E (m)	UTM-N (m)	Depth (m BGS)
well 003	671172	1517253	-104
well 005	684598	1535858	-161
well 009	668413	1527730	-227
well 012	664143	1525988	-201
well 015	657655	1523663	-220
well 018	644387	1525972	-113
well 019	662667	1508372	-171
well 021	677598	1533043	-229
well 024	671578	1532256	-57
well 025	658374	1522528	-101
well 026	658379	1522525	-165
well 028	678440	1523165	-112
well 032	678804	1520122	-165

Well NO.	UTM-E (m)	UTM-N (m)	Depth (m BGS)
well 088	669928	1520413	-169
well 125	632533	1524893	-194
well 131	638799	1544901	-291
well 132	635186	1563490	-225
well 140	638030	1520113	-195
well 144	661900	1531500	-101
well 147	640500	1534700	-104
well 151	654100	1531200	-234
well 152	644684	1532410	-207
well 155	652547	1526141	-261
well 159	654300	1538500	-109
well 162	666800	1537900	-110
well 166	660255	1548134	-213

Table 3.1 Locations of groundwater monitoring wells. (continued)

Well NO.	UTM-E (m)	UTM-N (m)	Depth (m BGS)
well 034	649742	1505389	-104
well 035	649787	1505439	-173
well 039	656637	1509921	-105
well 041	656625	1506172	-156
well 045	651849	1512198	-143
well 049	679603	1526824	-223
well 050	683153	1521422	-99
well 054	676757	1514161	-181
well 057	657347	1516550	-156
well 059	688318	1528358	-217
well 060	688401	1528351	-143
well 062	665391	1515354	-159
well 065	665018	1522040	-57
well 071	687617	1521775	-145
well 072	687599	1521797	-108
well 075	689762	1520081	-201
well 076	671983	1529008	-169
well 077	672788	1524331	-99
well 082	676333	1538220	-198
well 083	694919	1531872	-196

Well NO.	UTM-E (m)	UTM-N (m)	Depth (m BGS)
well 168	662011	1541561	-267
well 173	674037	1557553	-192
well 177	674437	1551869	-115
well 180	674804	1562460	-156
well 182	686897	1561028	-156
well 184	693665	1553159	-113
well 187	685228	1540814	-190
well 190	664323	1557028	-116
well 196	696893	1563413	-227
well 248	674575	1498368	-158
well 260	690317	1495168	-293
well 263	672755	1504137	-217
well 265	694548	1511799	-146
well 275	693541	1503372	-82
well 276	688407	1505900	-200
well 279	682776	1509087	-140
well 281	685080	1510700	-116
well 284	684373	1504888	-211
well 285	664473	1511249	-97
well 292	637500	1511000	-156

3.3 Conceptual model setting up

As described earlier, a conceptual model is a representative of the real system that consists of concepts. The conceptual model is often ideal and simple model that can help modeler to understand and simulate the system. Generally, the conceptual model determines the dimension and design the grid of model. The conceptual model must include boundaries and hydrologic unit. In this study, a conceptual model was constructed using hydrogeologic cross-sections obtained from JICA (1995). Four cross-section lines are presented in Figure 3.3. The surface elevation and JICA's cross-sections were used to conceptualize the hydrogeologic profiles that were used to establish the conceptual model. It should be noted that all conceptual models typically contain uncertainty because it is not possible to represent every detail of a hydrologic system even in a simple aquifer system.

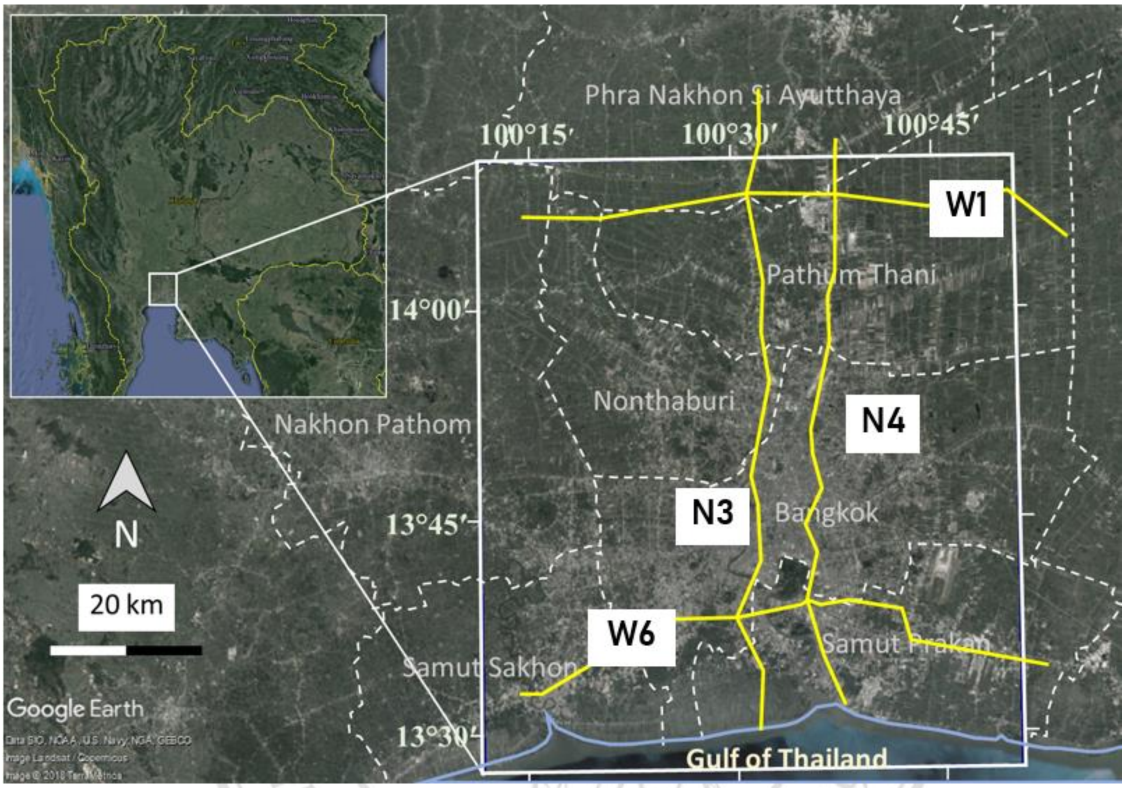

Figure 3.3 Cross-section lines (JICA, 1995).

Since this study focused on land subsidence simulation caused by groundwater extraction, thus the modeling depth was emphasized from ground surface to 300 m below ground surface (BGS) where major aquifers were extracted for groundwater and land subsidence occurred. In addition, deep aquifers extraction and subsidence have not been reported and the deeper data are not available. Thus, only the top four Bangkok's complex aquifer system were conceptualized, modeled, and simulated. Each of these aquifers has several interbedded clay layers that are prone to land subsidence. Figure 3.4 shows hydrogeologic cross-section of the N4 line. The top soft and stiff clay layers are defined as clay material. The gravel, sand, and clay sediment in the same aquifer (JICA, 1995) were grouped to the material namely Bangkok (BK), Phra Pradaeng (PD), Nakhon Luang (NL), and Nonthaburi (NB) aquifers. The hydrogeologic profile of N4 line can be conceptualized as shown in Figure 3.5. All of conceptualized cross-sections in model domain are shown in Figure 3.6.

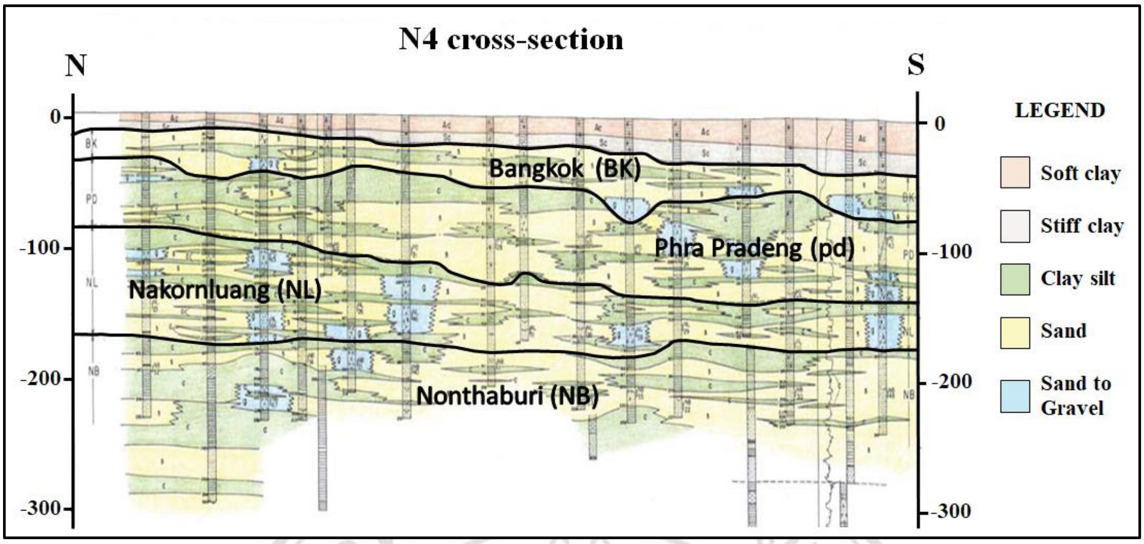

Figure 3.4 The N4 cross-section profile.

After simplifying the hydrogeology by grouping some of the similar aquifer materials, the conceptualized cross-sections were interpolated and extrapolated to obtain a solid model as shown in Figure 3.7. The conceptual or solid model has 5 layers. The top of model is in range of more than 10 to 0.3 m above mean sea level. The bottom of model is 300 m below mean sea level. The model covers area from 640,000 to 690,000 UTM-E and 1,549,000 to 1,568,000 UTM-N. The conceptual model will subsequently be transformed into a numerical model.

3.4 Numerical model setup

The numerical (or finite-difference) model was converted from the previously defined conceptual or solid model. MODFLOW (Harbaugh *et al.*, 2000; Harbaugh, 2005), computer code was used in this step onward.

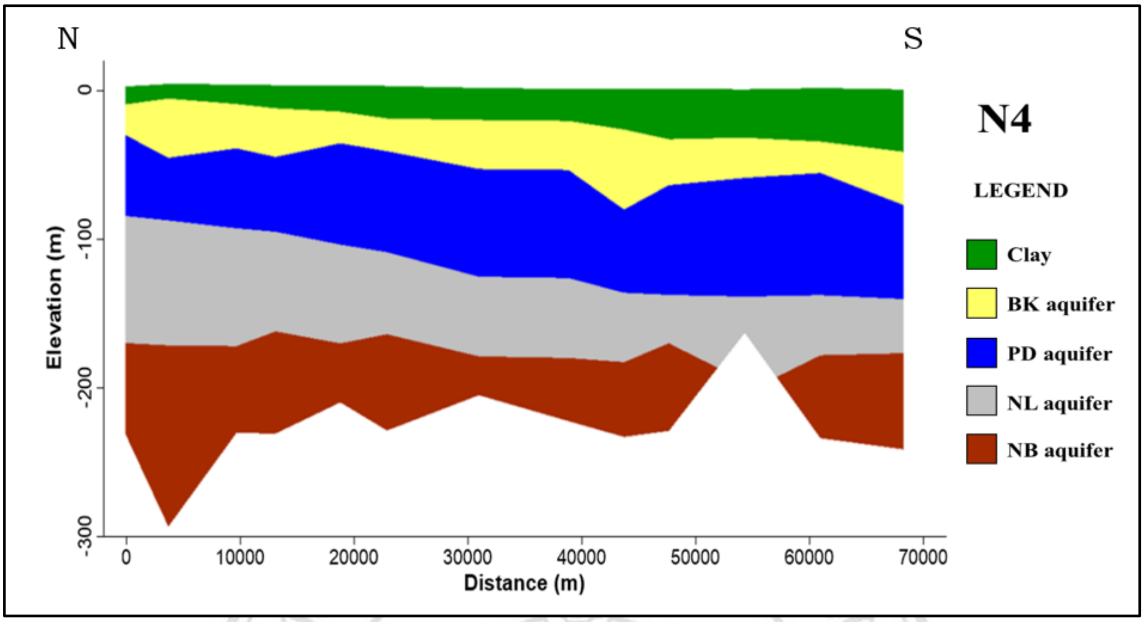

Figure 3.5 Conceptualized cross-section of the N4 line.

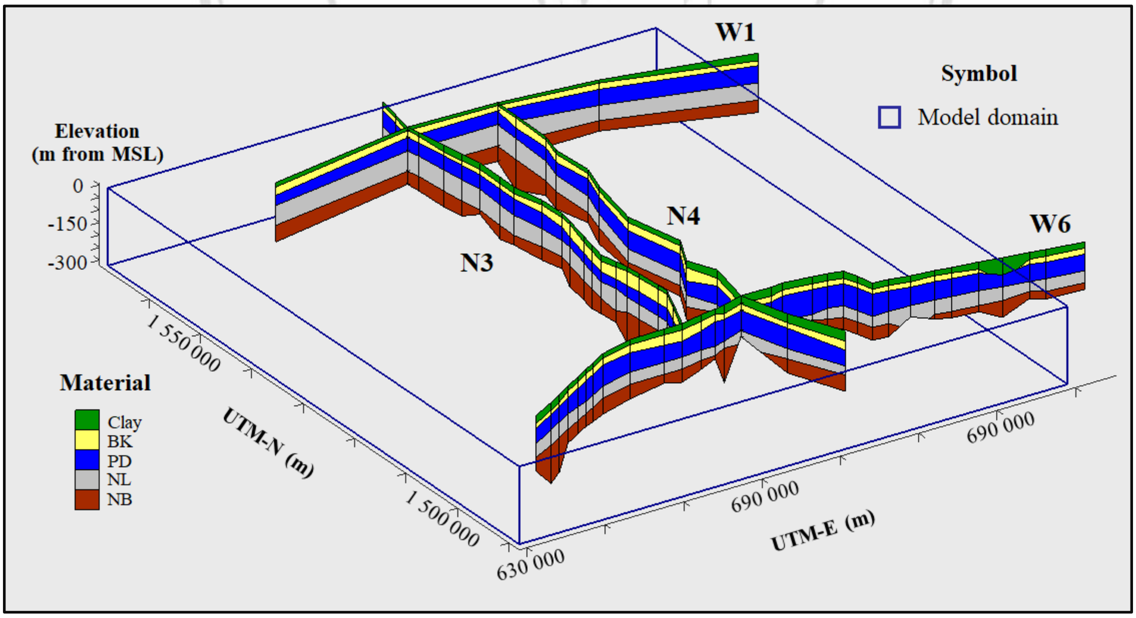

Figure 3.6 All of conceptualized cross-sections.

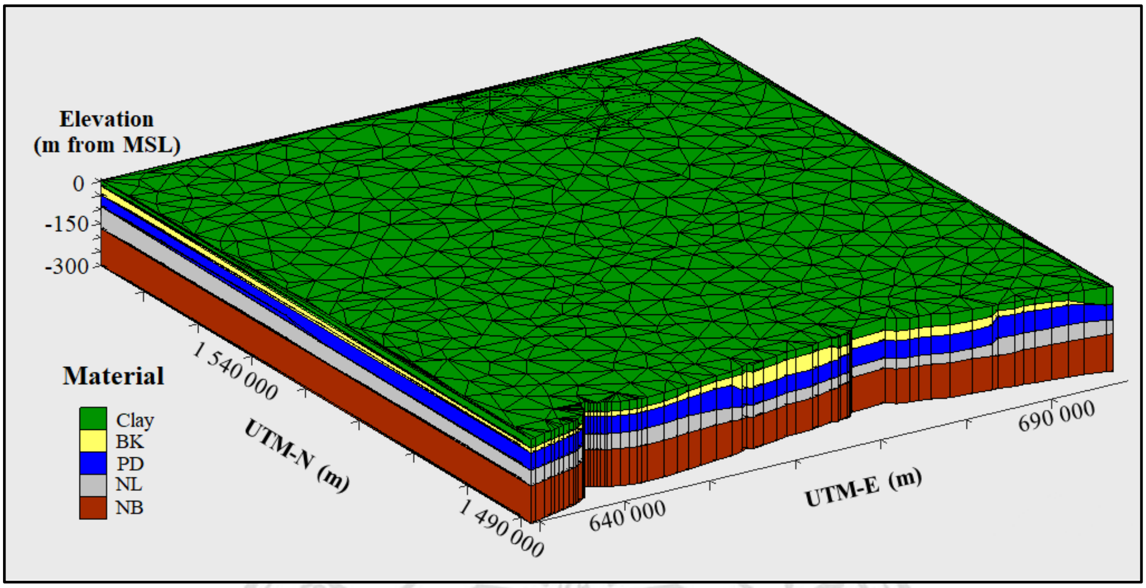

Figure 3.7 Conceptual or solid model.

3.4.1 MODFLOW program

MODFLOW program is a numerical program that approximates the hydraulic head solution of a groundwater flow equation. In three-dimension finite-difference model, the space or solid model is discretized into a parallelepiped grid blocks or cells. The *x*-direction blocks are called columns (I) that starts numbering from the left to right whereas the *y*-direction blocks are called rows (J) that starts numbering from upper edge to lower edge (top view), and the *z*-direction blocks are called layers (K) that starts numbering from top to bottom. The size of each grid block can be varied. The approximated hydraulic head represents hydraulic head at the center point of a grid block. Aside from space discretization, time is also discretized to the fundamental component called time steps. Time steps are grouped into stress period. The time-varying parameters can be changed every stress-period. MODFLOW code is designed to simulate either steady-state or transient conditions. In steady-state condition, time length is not affected to the solution head but it cannot be zero. Commonly the first stress period is steady-state and its solution is used as the initial condition of the following transient stress period. However, stress period conditions can be in any order.

MODFLOW can simulate several types of boundary conditions that allow groundwater exchange between internal and external source/sinks. These boundary conditions can be used together that are called “packages” in MODFLOW. This study uses eight packages that can be briefly described below and summarized in Table 3.2.

1. The Layer-Property Flow (LPF) package defines the horizon hydraulic conductivity (K_h) and the option for vertical hydraulic conductivity (K_v) or vertical anisotropy of the grid blocks. MODFLOW computes each conductance and groundwater flow using K values and grid geometry. This package also calculates the storage of groundwater system.

2. The Evapotranspiration (EVT) package is used to simulate how water is removed from cell by evaporation and plant transpiration.

3. The General-Head Boundary (GHB) package is used to simulate effect of far boundary head on model. The GHB package allows users to simulate a large regional model by chopping the model domain and replace with head-dependent flux boundary (McDonald and Harbaugh, 1988).

4. The Multi-Node Well (MNW2) package is used to simulate the well in multiple aquifers or a heterogeneous aquifer, partially penetrating wells, and horizontal wells (Konikow *et al*., 2009).

5. The Recharge (RCH) package is used to simulate groundwater recharge due to infiltration. The recharge value represents the amount of water that naturally or artificially fills the aquifer system. It should be noted that recharge is typically not equal to precipitation.

6. The river (RIV) package is used to simulate the water exchange between river and groundwater system.

7. The Inter-Bed storage (IBS) package is used to stimulate compaction and extension using groundwater level and aquifer’s elastic and inelastic properties. MODFLOW calculates subsidence or rebound by gathering the compaction or extension in each layer.

8. The Geometric Multi-Grid (GMG) solver is used to solve the system of linear equations from the finite-difference formulation in each time step of a MODFLOW stress period.

Table 3.2 The MODFLOW packages used in this study.

Package	Description
1. LPF	performs each grid storage and flow, input layer type and grid properties such as hydraulic conductivity and storage coefficient (or storativity)
2. EVT	simulates evapotranspiration (ET) rate, input Max ET rate and extinction depth
3. GHB	simulates effect of boundary head, input boundary head and conductance
4. MNW2	defines the wells that exist in more than one cell, input extraction rate
5. RCH	represents water that fill the groundwater system, input recharge flux
6. RIV	simulates the river type boundary condition, input river bed conductance
7. IBS	simulates layer compaction or extension, input preconsolidation head, skeleton component of elastic and inelastic specific storage
8. GMG	solves the finite-different equation in each step

3.4.2 Model grids

The study area is located on the Central Thailand plain. It covers 5,600 km^2 with 70-km width (East-West direction) and 80-km length (North-South direction). The model is discretized to the uniform numerical grid block with the size of 2000×2000 m^2 ($\Delta x \times \Delta y$). There are some inactive cells or blocks in southern part of the model because the grids lie within the Gulf of Thailand. The finite-difference grid is shown in Figure 3.8 and Figure 3.9. The model contains five 'heterogeneous' aquifer materials that are top clay (clay) unit, Bangkok (BK) aquifer unit, Phra Pradaeng (PD) aquifer unit, Nakhon Luang (NL) aquifer unit, and Nonthaburi (NB) aquifer unit. It should be emphasized that, each of the modeled aquifers are heterogeneous even though Figure 3.9 shows only five colors for five materials. All layers of model are set as convertible type that is changeable between confined or unconfined aquifer depending on groundwater level. The model was executed in a period of January 1, 2010 to June 1, 2016 where observed hydraulic heads were recorded and used as calibration targets.

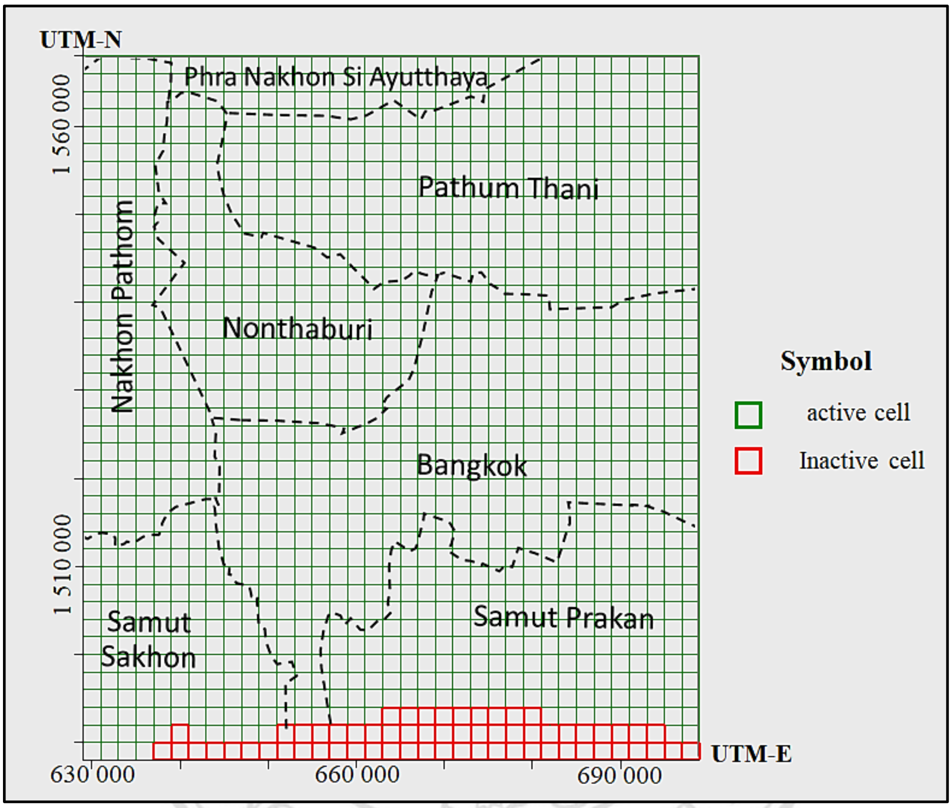

Figure 3.8 Numerical grid of study area (top-view).

3.4.3 Model parameters

The model input parameters consisted of hydraulic properties of heterogeneous aquifers as well as the boundary conditions. These parameters will be calibrated to ensure model fit are described below.

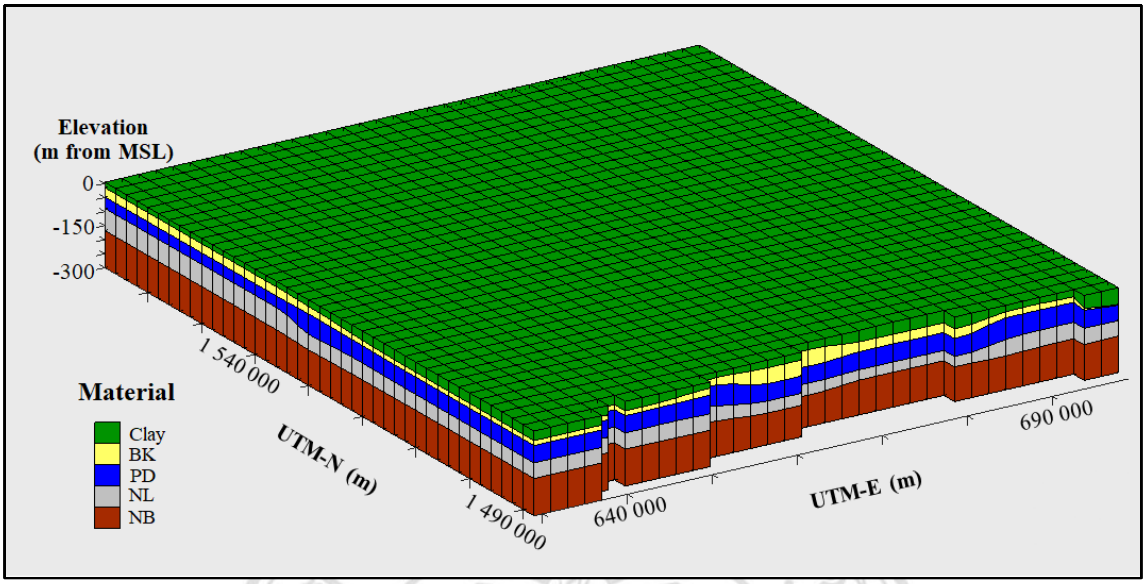

Figure 3.9 Finite-different grid used in this study.

1. Hydraulic properties of aquifer consist of hydraulic conductivity and storage coefficient. Hydraulic conductivity is the parameter that defines how groundwater flows through the grid cells. In this study, the values of horizontal hydraulic conductivity are obtained from available, but very limited, pumping tests data. These hydraulic conductivities for BK aquifer, PD aquifer, NL aquifer and NB aquifer are in the range of 1.9-98.2, 1.7-183.6, 1.8-147.4 and 1.8-161.6, respectively (JICA 1995). The hydraulic conductivity was initially assumed uniform of 1 m/d which may either be lower or higher than previously reported because aquifer units in this study are complex mixtures of gravel, sand and clay materials. However, as the calibration progressed, the initial value will be updated at the pilot points and interpolated into the finite difference grid blocks resulting a heterogeneous aquifer system. For top clay (or clay) layer the hydraulic conductivity is assumed 0.0001 m/d. The initial horizontal and vertical anisotropy (K_h/K_v) is unknown and, initially, assumed to have a value of 10. Storage coefficient (or storativity) is the volume of groundwater given up from aquifer per unit decline of hydraulic head per horizontal aquifer area or store. The storage coefficient data, similar to the hydraulic conductivities, are very limited. Thus, it is assumed that the specific storage and specific yield are 0.0001 m^{-1} and 0.1, respectively based on the suggested values from IBS package (Leake and Prudic, 1991). The model is, later, calibrated for S_s and S_y based on pilot points calibration for maintaining heterogeneity.

Table 3.3 Summary of model setup.

Model setting	Note
Unit	
- Length and thickness	m
- Time	d
- Hydraulic conductivity	m/d
- Conductance	m^2/d
- Pumping rate	m^3/d
- Recharge and ET rate	m/d
Model scope	
- E-W range (UTM-E)	629,000-699,000
- N-S range (UTM-N)	1,488,000-1,568,000
- Width	70,000
- Length	80,000
- Bottom and top (from MSL)	-300 to ~10
Space setting	
- Grid size (E-W)	2000
- Grid size (N-S)	2000
- Number of columns	35
- Number of rows	40
- Number of layers	5
- Thickness of layer	variable
- Number of cells	6685 active and 315 inactive
Time setting	
- Model period	1st January 2010 to 1st June 2016
- Steady-state condition period	1st January 2010
- Transient condition period	2nd January 2010 to 1st June 2016
- Stress period	1 month

2. Recharge's main source is an infiltration of precipitation. Typically, recharge flux is approximately 10% of precipitation but the study area is discharge zone where recharge is low. The study area, covering seven provinces, generally has low natural recharge ranging from 5 to 150 mm/yr precipitation due to a thick covering clay layer (Faculty of Engineering Chulalongkorn University, 2009). In modeling groundwater flow, the recharge was initially assumed uniform. However, during model calibration based on pilot points method, the recharge values will be non-uniform. In Bangkok, the average of annual rainfall in a period of 2003 to 20015 is about 1,600 mm and average rainy duration is about 120 d (NSO, 2016). In transient simulation, recharge flux is assigned in a period of May to August and flux in each stress period.

3. Evapotranspiration (ET) consists of direct evaporation and plant transpiration. The evapotranspiration rate depends on depth of piezometric surface and depth of root plant that depends on species of plant. The evapotranspiration rate linearly decreases with depth. The "extinction depth" is the depth without effect of evapotranspiration. This study estimated the extinction depth as 5 m that is the average depth of plant roots in sandy clay to clay (Shah *et al*, 2007) and maximum of evapotranspiration of approximately 750-800 mm/yr in cultivation area in Tha Chin and Mae Klong river basin (Panya Consultants Co., Ltd, 2009). Similar to hydraulic parameters and recharge, the evapotranspiration rate will be calibrated based on pilot points method allowing a non-uniform ET distribution.

4. River can be source or sink of groundwater depending on groundwater head and water level or stage in river. There are two major rivers in the study area. The first one is Chao Phraya river in the center and another one is Tha Chin river in the western part. The rivers are modeled by RIV package and flow between river and aquifer is controlled by river-bed conductance. The riverbed conductance is not known, thus its values are assigned as 10 m^2/day for both rivers and will be calibrated for suitable value later. Figure 3.10 shows the RIV package of Chao Phraya river (middle) and Tha Chin river (left side).

5. Constant head and general-head boundary condition represent the exchange between internal model and external model. The southern boundary of the study area connects with the Gulf of Thailand so this boundary is defined as constant head boundary. The constant head value is assigned constant value as 0 m from mean sea level (MSL). The other boundaries, which are northern, eastern, and western boundaries, are determined as general-head boundary (GHB) that represent the faraway boundary head. The water exchange in GHB package is controlled by boundary head and conductance that depend on hydraulic conductivity and area of cell perpendicular to flow direction and distant from boundary head ratio. In this study, the initial conductance is assigned as 10 m^2/day. The Figure 3.11 show boundary condition of model.

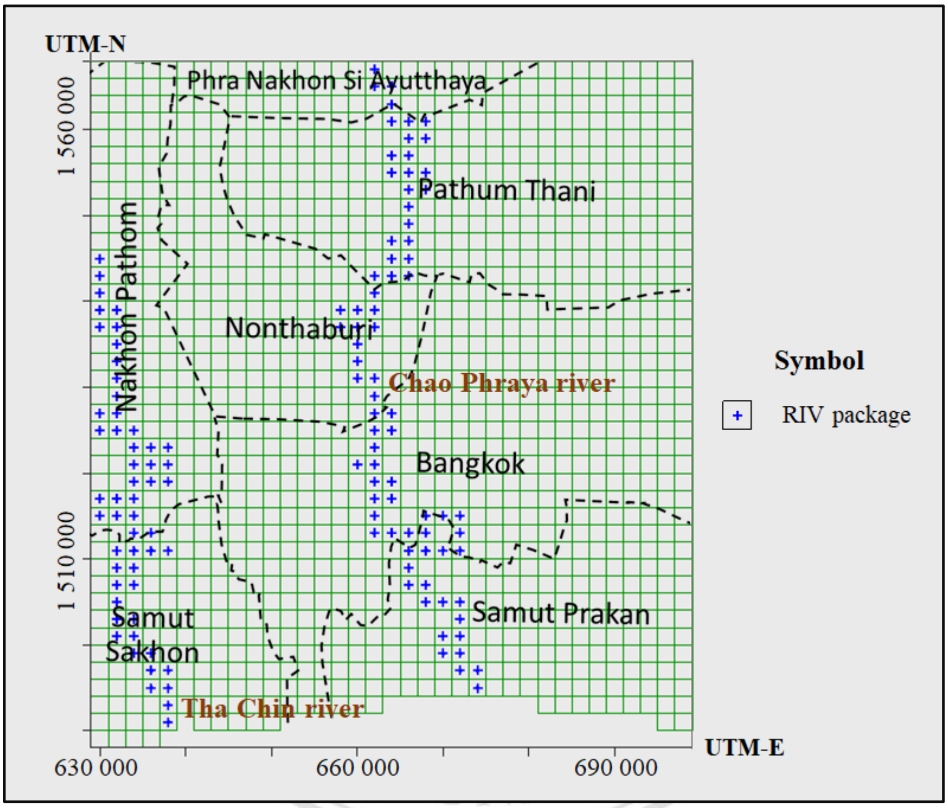

Figure 3.10 River location in numerical model.

6. Groundwater extraction is the main cause of groundwater level decrease. In Bangkok, the pumping rate is as large as 30,000-70,000 m^3/d for the model area. Most of extraction well drains the groundwater from depth less than 300 m BGS. There are about 600 active pumping wells that are officially registered. In this study, the MNW2 package is used to represent the pumping well. The MWN2 package allows the multiple screen intervals of the pumping wells. Users need to assign the total pumping rate and the model will automatically assign the extraction rates for each of the intervals. Figure 3.12 shows location of pumping well and MNW2 package.

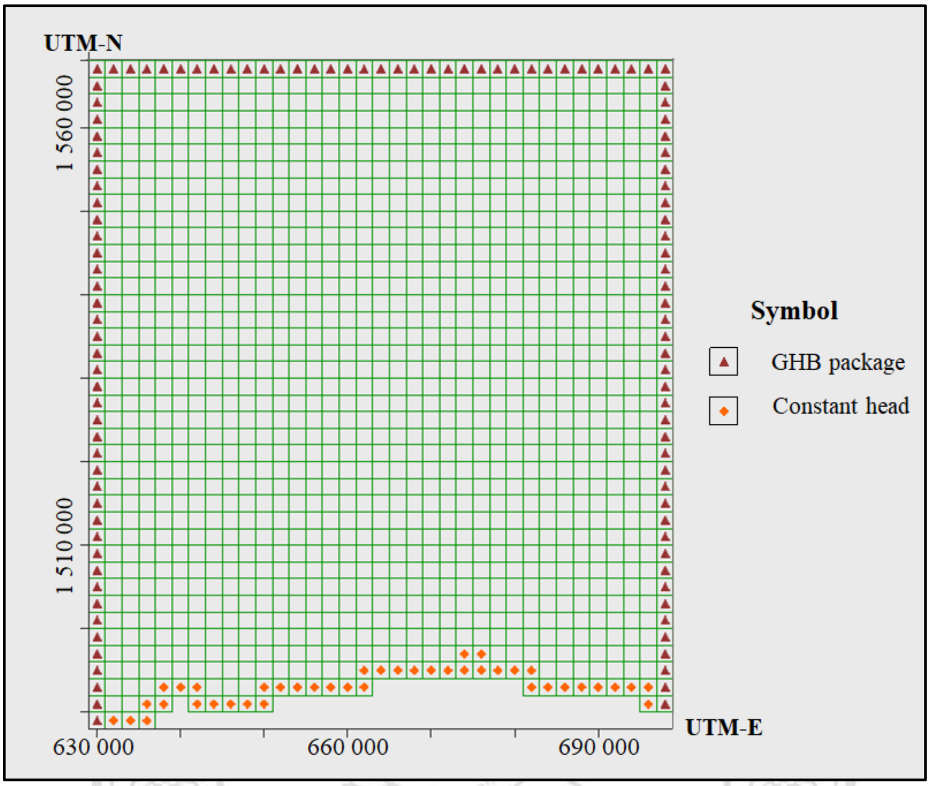

Figure 3.11 Boundary of model.

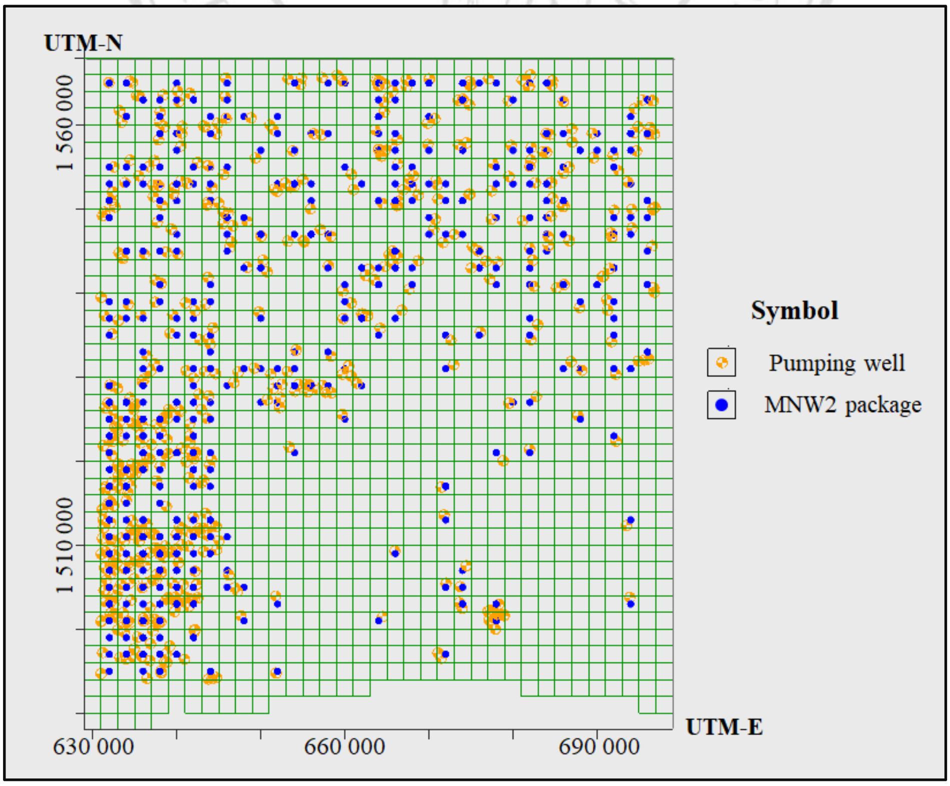

Figure 3.12 Pumping well and MNW2 package.

3.4.4 Model calibration

Model calibration is the process of adjusting model parameters to match the computed to observed heads in order to represent the real system as much as possible. In the past, the model was calibrated manually by trial-and-error procedure that started with assuming the initial model parameters before run the model. Next, the simulated result was compared with the observation data. If the simulation is not satisfied, the parameters will be changed or updated and model will be executed again. These processes are repeated until the acceptable results are obtained. However, the model parameters must in range of reasonable and realistic. The disadvantage of this method is time-consuming when the model contains a large number of parameters. The automated parameter estimation is based on reducing the objective function (sum of squared errors, SSE or Φ) which collectively indicates the level of matching between simulation results and observation data. The sum of squared errors (SSE or Φ), which also known as residual sum of squares (RSS) or sum of squared residuals (SSR), is usually used as objective function. The sum of square errors for N observations can be written as:

$$SSE \text{ or } \Phi = \sum_{i=1}^{N} \omega_i (x_i - \hat{x}_i)^2 , \tag{3-1}$$

where $\hat{x}_i$ is the model simulated values, x_i is the observed or measured values and ω_i is the weight of the measurement. The higher value of SSE means the higher error between simulated values and observation. PEST (Doherty, 1994), which is the automated parameter algorithm, is used to calibrate and estimate model parameters in this study. The parameter values will be systematically and automatically updated in each iteration based on the calculated sensitivity values. The sensitivity of parameter P_j (or $\partial\Phi/\partial P_j$) is calculated by the difference in SSE or Φ evaluated before and after changing in the value of parameter (or $\Phi(P_j + \Delta P_j) - \Phi(P_j)$) divided by change in parameter value (ΔP_j) as shown in equation (3-2) which is an example of forward difference operation.

$$\frac{\partial\Phi}{\partial P_j} = \lim_{\Delta P_j \to 0} \frac{\Phi(P_j + \Delta P_j) - \Phi(P_j)}{\Delta P_j} \approx \frac{\Phi(P_j + \Delta P_j) - \Phi(P_j)}{\Delta P_j} , \tag{3-2}$$

The highly sensitive parameter has higher effect on model than parameters of lower sensitivity. PEST has a dedicated sensitivity analysis module that records and compares the simulated results when parameter change. Insensitive parameter(s) will not be adjusted during iterations. Pilot point model calibration technique is used in calibration process. Highly (spatially) heterogeneous model can be more beneficial from the pilot point than traditional parameter zonation which calibrates single parameter value for entire zone. The pilot point technique adjusts parameter at every pre-defined point and each point has its individual value. The parameter values are interpolated between points that made the value of parameter varying from cell to cell. In the past, pilot point technique cannot be used when the number of parameters is greatly exceeding observation number. In later version, PEST provide the pilot point option called "regularization" that adjust weight of parameter or add "regularization term" to objective function. As a result, the model reliability and stability will be increased significantly. With regularization, the number of parameters is greater than the number of observations. The more complicated of parameter value distribution leads to lower error. For the location of certain parameters, pilot point can also be fixed at specific values called "fixed pilot point."

There are eight sets of model parameters for calibration: hydraulic conductivities, vertical anisotropies, specific storage, specific yield, recharge fluxes, maximum evapotranspiration rates, river-bed conductance, and general-head conductance. Pilot point method is used to calibrate spatially variable parameters such as hydraulic conductivity, specific storage, specific yield, recharge flux and maximum evapotranspiration rate. There are 56 pilot points in each model layer (approximately one pilot point per 10 km^2). Locations of a pilot point set are shown in Figure 3.13. Table 3.4 summarizes initial parameter values used as starting input parameter values. It should be noted that although the pilot point calibration starts with uniform model parameter values, their updated values (during calibration iteration) are limited or confined within the values obtained from field pumping tests (if available). After calibration, the parameter values will no longer be uniform and the field becomes heterogeneous.

The calibration targets for flow model included observed heads from 66 observation wells as shown in Figure 3.2. All of observation wells are assumed to have the same reliability (i.e. same weights). The steady-state model is also used to calibrate the groundwater extraction rate by three multipliers include 0.625, 1.0, and 1.5 that are the representative of groundwater extraction in model that are lower, equal, higher than the report. the best multiplier is used in transient condition.

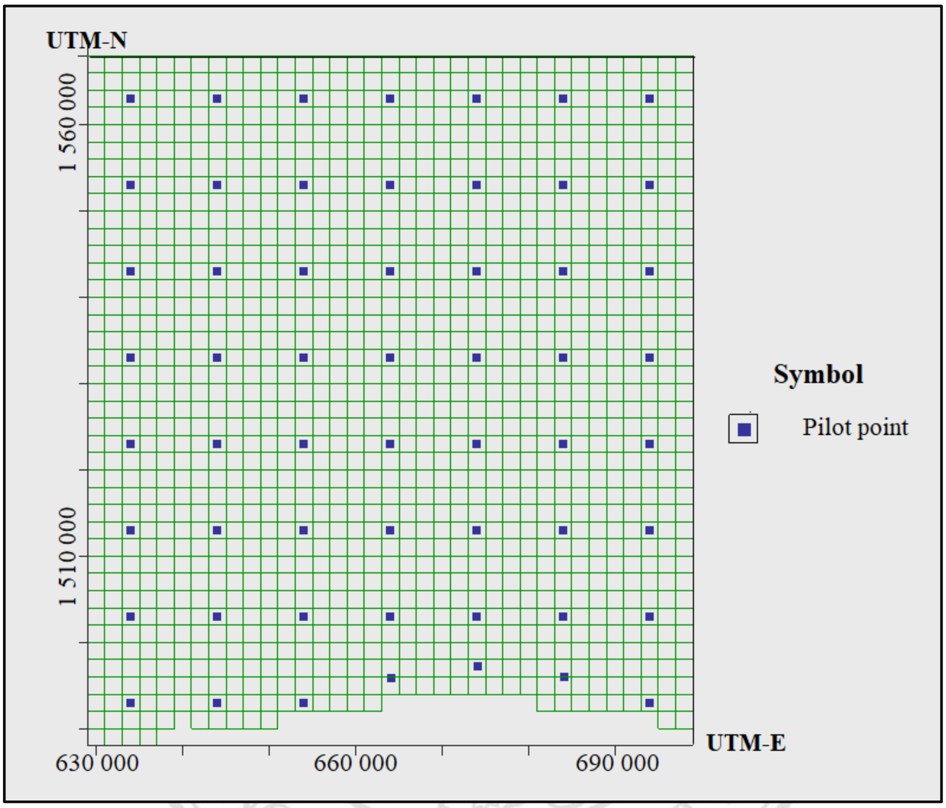

Figure 3.13 Pilot point location.

3.5 Land subsidence modeling and calibration

After the flow model was successfully calibrated, it was subsequently used to simulate land subsidence. The IBS package is activated. The preconsolidation head distribution was assigned. The initial skeleton components of elastic and inelastic specific storage values were not known, thus they were initially assumed to be uniform with the values of 0.0001 and 0.00001 m^{-1}, respectively. The land subsidence model was simulated during a period of January 2010 to June 2016. The subsidence model was calibrated manually for elastic and inelastic coefficients based on 37 subsidence observation points shown in Table 3.5. The subsidence observation data used in this study is in a period of 2010-2012 (Chaithavee 2015) and 2014 and 2016 (DGR 2018). After calibration, the model was used to predict subsidence/rebound for the next 20 years.

Table 3.4 Summary of initial parameter.

Parameter		Initial value	Note
Hydraulic conductivity	clay	0.0001 m/day	pilot points
	aquifer	1.0 m/day	pilot points
vertical anisotropy		10	-
Specific storage	clay	0.0001 m^{-1}	pilot points
	aquifer	0.0001 m^{-1}	pilot points
Specific yield	clay	0.1	pilot points
	aquifer	0.1	pilot points
River-bed conductance	Chao Phraya	10 m^2/day	-
	Tha Chin	10 m^2/day	-
GHB conductance	west	10 m^2/day	-
	east	10 m^2/day	-
	south	10 m^2/day	-
Recharge		0.0001 m/day	pilot points
Maximum ET		0.0001 m/day	pilot points

Table 3.5 Location of subsidence observation.

Observe Points	UTM-E (m)	UTM-N (m)
SUB_OB01	676927	1533547
SUB_OB02	687239	1527863
SUB_OB03	686299	1512643
SUB_OB04	673881	1547360
SUB_OB05	689280	1541165
SUB_OB06	696872	1540663
SUB_OB07	696765	1542919
SUB_OB08	682222	1524879
SUB_OB09	674490	1551801
SUB_OB10	676554	1497332
SUB_OB11	673984	1500159
SUB_OB12	674036	1500879
SUB_OB13	673487	1546357
SUB_OB14	679862	1547790
SUB_OB15	682333	1548363
SUB_OB16	676966	1506687
SUB_OB17	678713	1505968
SUB_OB18	680616	1505454
SUB_OB19	682569	1504991

Table 3.6 Location of subsidence observation. (continued)

Observe Points	UTM-E (m)	UTM-N (m)
SUB_OB20	668156	1509713
SUB_OB21	668666	1527724
SUB_OB22	662469	1507870
SUB_OB23	680410	1496818
SUB_OB24	687453	1493836
SUB_OB25	685499	1494196
SUB_OB26	688886	1541201
SUB_OB27	689137	1540914
SUB_OB28	663497	1506071
SUB_OB29	663909	1504374
SUB_OB30	677065	1516361
SUB_OB31	676418	1516662
SUB_OB32	679708	1530466
SUB_OB33	675506	1532731
SUB_OB34	672400	1534266
SUB_OB35	675493	1541129
SUB_OB36	674669	1538300
SUB_OB37	682749	1517673

CHAPTER 4

RESULTS AND DISCUSSION

4.1 Groundwater flow simulation

This section illustrates and discusses the steady-state and transient groundwater flow models.

4.1.1 Steady-state simulation

The steady-state groundwater flow model is used to simulate groundwater system under the equilibrium condition such as long-term constant rate of groundwater pumping or insignificantly changing in groundwater storage (Anderson *et al*., 2015). The steady-state model is used as primary calibration for hydraulic conductivity, maximum evapotranspiration rate, river-bed conductance, general head conductance, and sensitivity analysis. The model is also used to evaluate realistic groundwater extraction rates, hydraulic conductivities, vertical anisotropy, maximum evapotranspiration rate, river-bed conductance, general-head conductance as described in Chapter 3.

The steady-state model in aquifer system was setup and simulated by MODFLOW (Harbaugh *et al.*, 2000; Harbaugh, 2005) and then the model was calibrated using PEST algorithm (Doherty, 1994 and Doherty, 2003). The calibration target refers to a set of hydraulic head data measured at 66 observation wells. The difference between calculated and observed head is called error or residual. In this study, the acceptable error of calculated head is set as ±2 m. Figure 4.1 shows the calibration target with error bar. The center of target is observed or measured head value. The range of the target is the acceptable error interval. The bar length represents the residual of simulation head. The color of bar presents the magnitude of residual. When the bar is green, the error is smaller than upper/lower limit of acceptable error. If the error is in range of 100-200%, the bar is yellow. And the bar is red when residual exceeds 200% of calibration target.

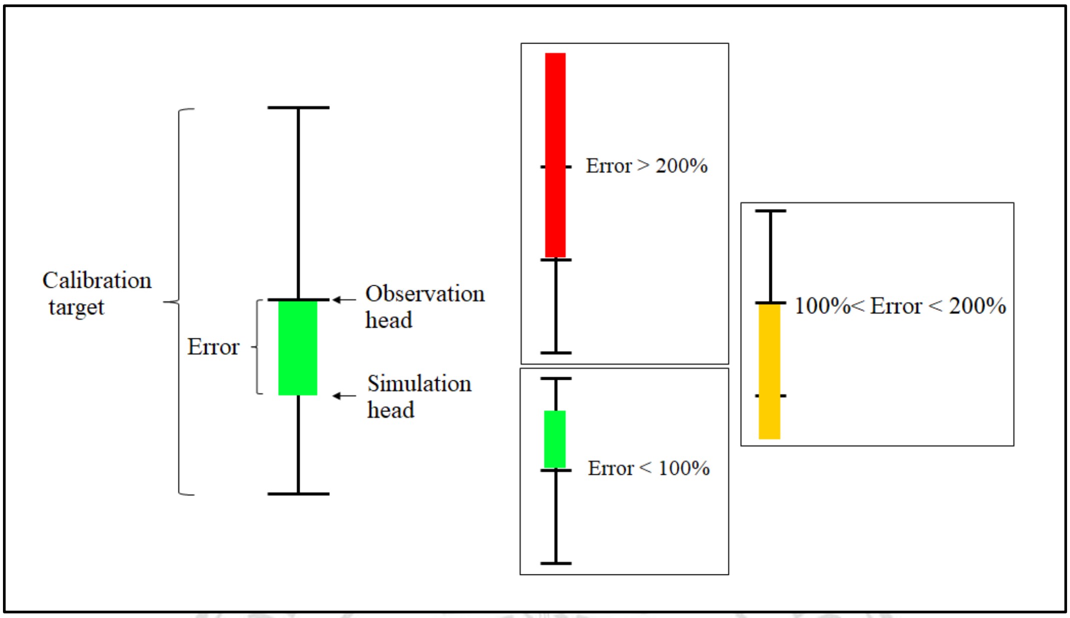

Figure 4.1 calibration target.

With pilot point technique and regularization, PEST (Doherty, 1994 and Doherty, 2003) allows the model to be heterogeneous within a zone. This technique is very efficient but takes relatively long period of execution time. Since the actual pumping rates are not known and the reported pumping rates are always underestimated due to the existence of unregistered/unreported groundwater wells. The pumping rates were also calibrated using multiplier as a parameter. The smallest root-mean squared error (RMSE) between observed and calculated heads was used to decide the best multiplier value which, after calibration, turned out to be 1.50.Table 4.1 shows simulated and observed heads at observation wells from steady-state simulation. Figure 4.2 shows the comparison of the calibrated steady-state head with observation head. The values of calculated heads are relatively comparable to the observed heads except for the well 260 where the calculated value is different from observation value as 13.31 meters of which the cause of discrepancy must further be investigated.

Table 4.1 Simulated and observed hydraulic heads from steady-state model calibration.

Well	Head (m)		Residual	Well	Head (m)		Residual
	observed	simulated			observed	simulated	
well 003	-18.44	-17.28	1.16	well 088	-21.98	-20.43	1.55
well 005	-28.85	-29.24	-0.39	well 125	-35.92	-36.70	-0.78
well 009	-21.10	-22.20	-1.10	well 131	-15.83	-15.15	0.68
well 012	-20.46	-21.58	-1.12	well 132	-18.93	-18.92	0.01
well 015	-24.23	-22.88	1.35	well 140	-38.05	-36.21	1.84
well 018	-18.68	-19.84	-1.16	well 144	-15.72	-14.82	0.90
well 019	-20.51	-20.95	-0.44	well 147	-13.54	-14.60	-1.06
well 021	-23.47	-24.95	-1.48	well 151	-21.83	-22.05	-0.22
well 024	-13.67	-15.58	-1.91	well 152	-24.26	-23.26	1.00
well 025	-16.99	-16.87	0.12	well 155	-22.85	-23.28	-0.43
well 026	-21.05	-20.10	0.95	well 159	-13.57	-13.25	0.32
well 028	-15.85	-17.44	-1.59	well 162	-15.46	-18.47	-3.01
well 032	-25.64	-23.46	2.18	well 166	-19.61	-20.33	-0.72
well 034	-20.32	-20.16	0.16	well 168	-23.80	-21.79	2.01
well 035	-23.23	-23.43	-0.20	well 173	-22.23	-22.26	-0.03
well 039	-18.85	-19.08	-0.23	well 177	-23.41	-23.41	0.00
well 041	-20.47	-20.96	-0.49	well 180	-24.98	-24.94	0.04
well 045	-21.12	-21.98	-0.86	well 182	-24.98	-25.14	-0.16
well 049	-26.63	-26.97	-0.34	well 184	-37.10	-35.53	1.57
well 050	-16.09	-19.09	-3.00	well 187	-27.34	-28.11	-0.77
well 054	-23.16	-25.10	-1.94	well 190	-15.57	-15.89	-0.32
well 057	-20.48	-21.15	-0.67	well 196	-34.61	-34.39	0.22
well 059	-29.24	-28.29	0.95	well 248	-19.76	-15.67	4.09
well 060	-32.88	-28.94	3.94	well 260	-25.28	-11.97	13.31
well 062	-20.35	-20.76	-0.41	well 263	-21.23	-22.11	-0.88
well 065	-17.06	-16.77	0.29	well 265	-23.79	-26.27	-2.48
well 071	-26.37	-26.79	-0.42	well 275	-17.89	-19.03	-1.14
well 072	-23.19	-23.21	-0.02	well 276	-25.75	-25.62	0.13
well 075	-28.85	-28.09	0.76	well 279	-23.35	-22.20	1.15
well 076	-22.03	-19.69	2.34	well 281	-23.29	-22.62	0.67
well 077	-16.20	-17.01	-0.81	well 284	-24.32	-25.20	-0.88
well 082	-23.37	-23.72	-0.35	well 285	-18.42	-18.35	0.07
well 083	-27.44	-28.61	-1.17	well 292	-32.08	-32.21	-0.13

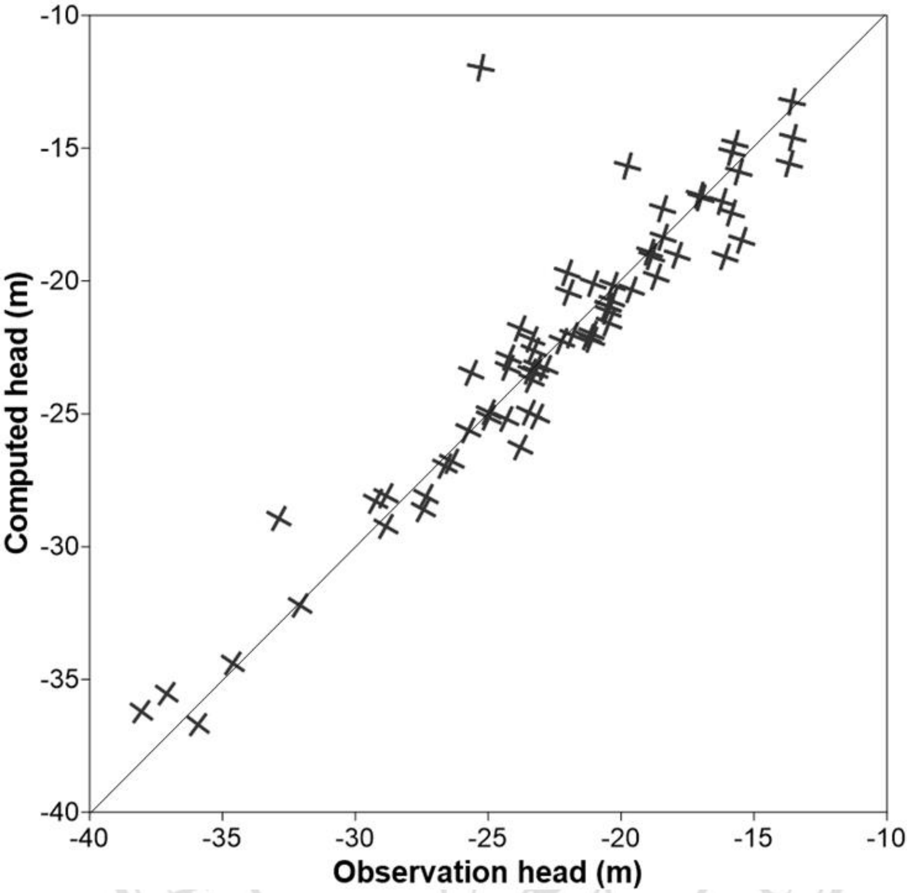

Figure 4.2 Simulated vs. observed hydraulic heads (steady-state simulation).

Figure 4.3 shows the hydraulic head distribution from steady-state calibrated groundwater flow model. The highest hydraulic head value is shown in blue and the lowest value is red. High hydraulic head zones are located near mid-western and northern boundary of layers 1 to 3. There are low hydraulic head zones in the upper part near the east boundary in layers 2 to 5 and the lower head zone near west boundary. The lower hydraulic head zone was caused by high groundwater extraction rate.

4.1.2 Transient simulation

Transient model is used to simulate time-dependent flow behavior of the aquifer system. The aim of transient calibration is to match the simulated heads to time series of observed values. The calibrated transient model can further be used to predict future hydraulic head distribution as well as subsidence simulation.

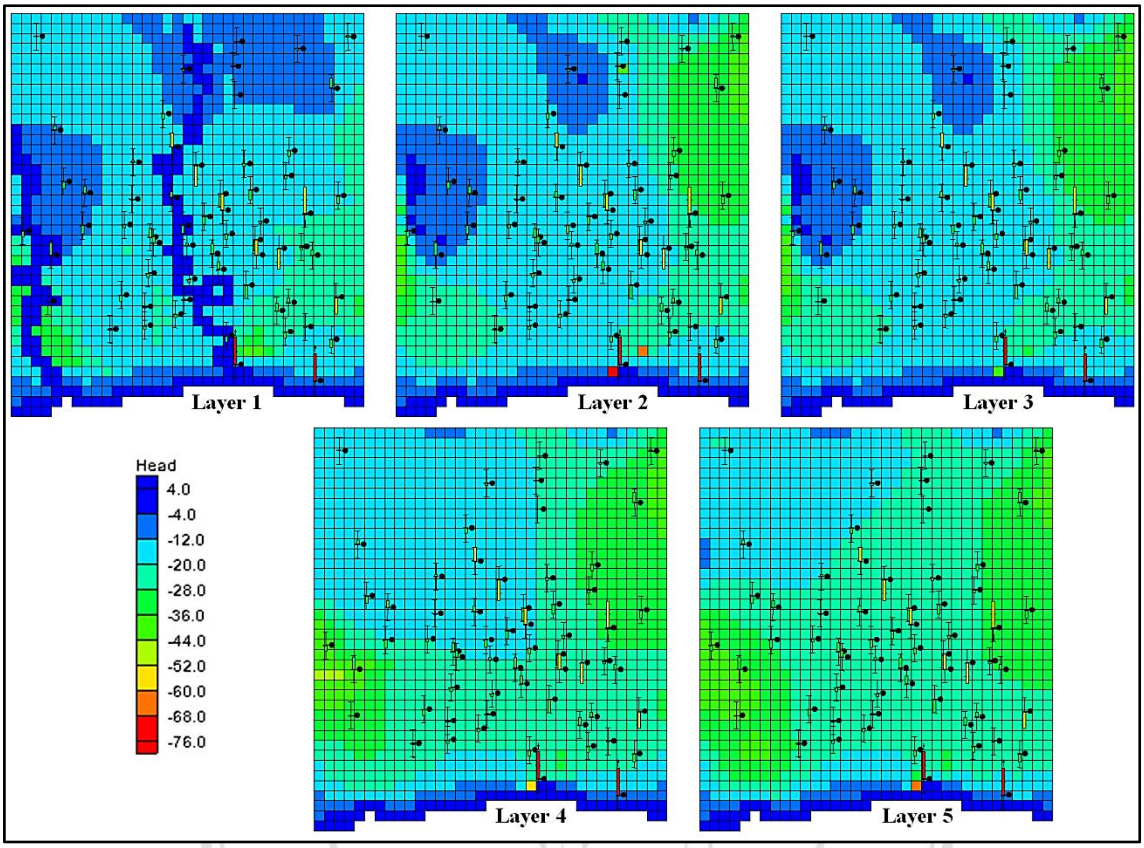

Figure 4.3 Calibrated steady-state head distribution from top (layer 1) to bottom (layer 5).

The calibrated steady-state groundwater flow model was used as initial condition of transient model. The calibrated steady-state head was used to starting head of transient simulation. The pumping rates were varying with time. Additional calibrated parameters include specific yield and specific storage of all model layers. Transient simulation is executed during a period of January 2010 to June 2016 (approximately 5 years and 5 months). Recharge flux is assigned during a period of May to August each year. Max ET rate is assumed constant. The transient simulation was divided to 77 stress periods. The duration of each period is one month. Stress periods were subdivided to 10 time-steps. The pilot point technique was used to calibrate the additional parameters which included specific storage, specific yield, and time-dependent recharge.

The results of calibrated transient groundwater flow model are illustrated in Figure 4.4 and Figure 4.5 which are the time series plot of simulated hydraulic heads versus observed heads for some selected wells during January 2010 to June 2016. The simulation demonstrates that it can capture aquifer's seasonal response or behavior relatively reasonable although some wells display either underestimated or overestimated heads.

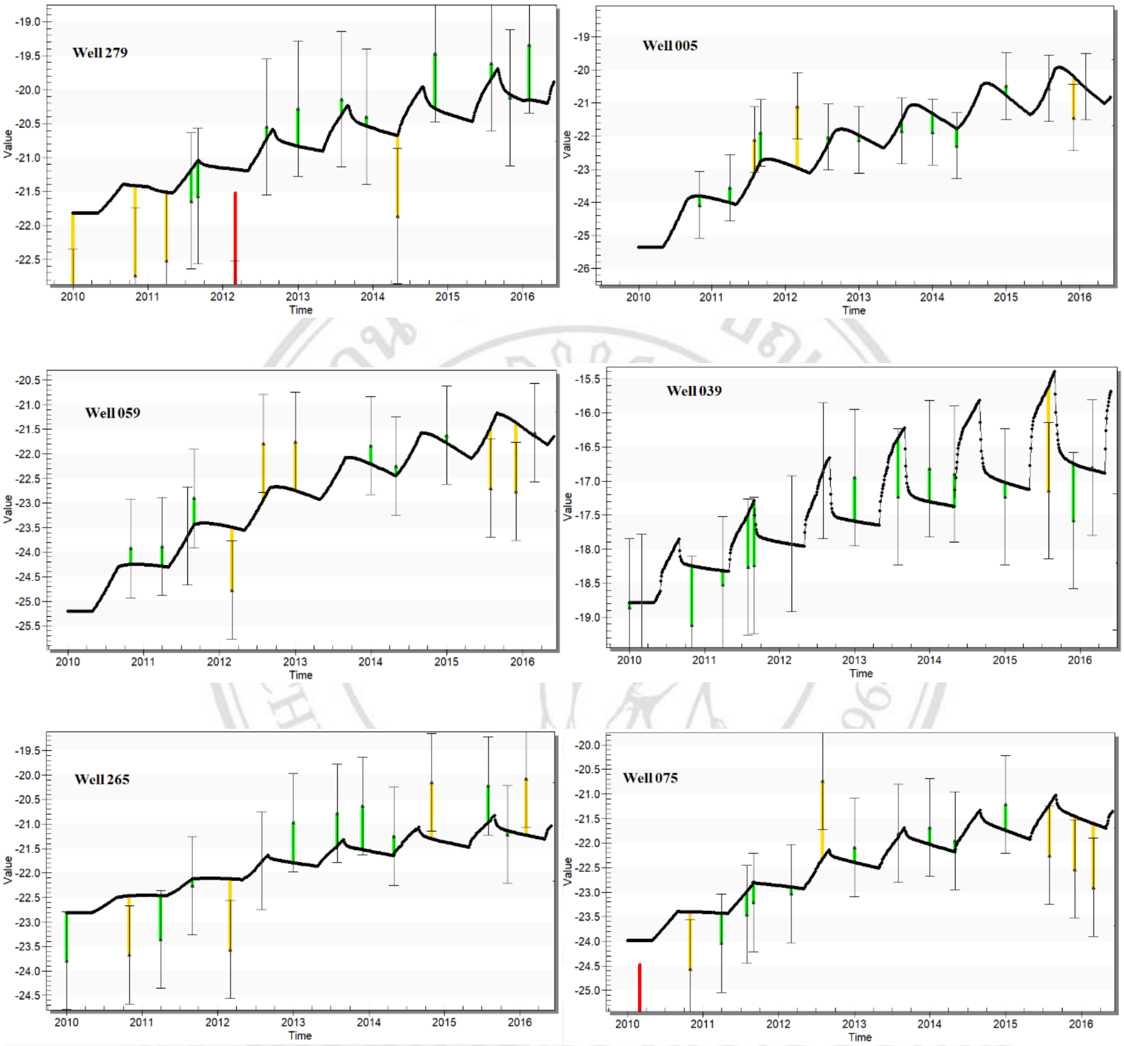

Figure 4.4 Examples of transient simulation results (relatively well-captured behavior).

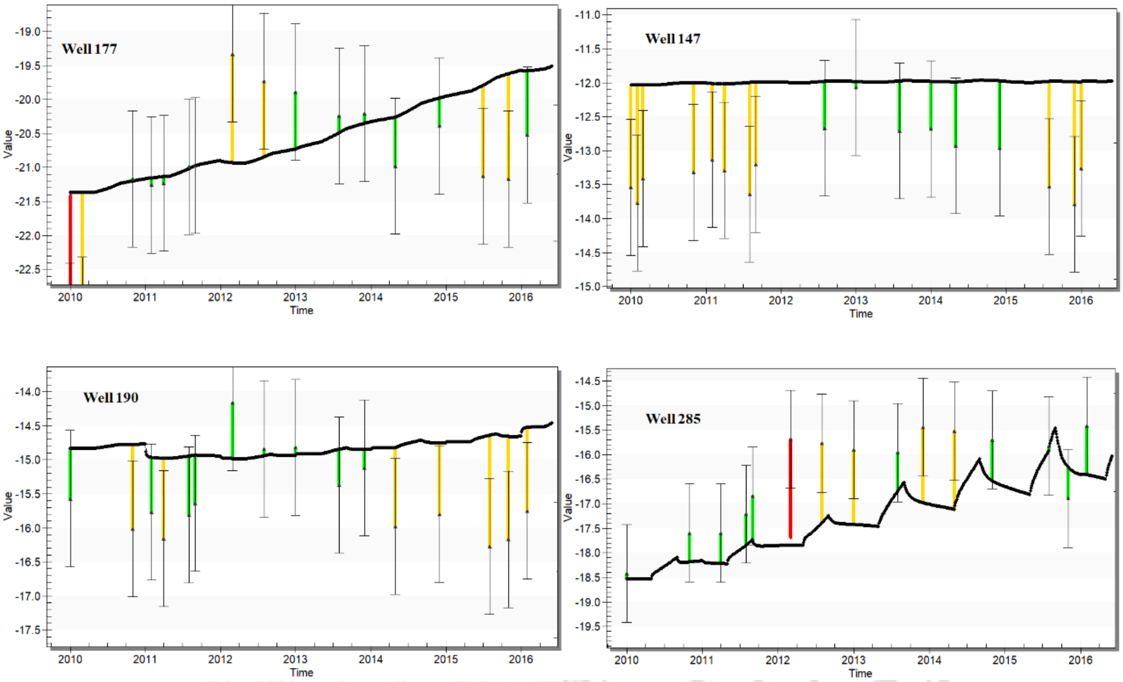

Figure 4.5 Examples of transient simulation results (either under- or over-estimated behavior).

Table 4.2 shows the final parameter values along with mean, median, minimum and maximum values obtained from steady-state model calibration. The hydraulic conductivity range is very wide with 5 to 6 order of magnitude and their distributions are positively skewed for all materials. There were only few numbers of data that are close to maximum so it was not necessary to increase the calibration upper boundary. The hydraulic conductivity value of clay material is apparently lower than aquifers and have high anisotropy indicating no vertical flow of groundwater. The evapotranspiration range is narrow indicating that homogeneous parameter zonation may be sufficient for future simulation. The recharge values are very low because study area is mainly a discharge groundwater zone. The riverbed conductance of Tha Chin river is slightly higher than Chao Phraya river with only one order of magnitude difference.

Figure 4.6 illustrates the distribution of hydraulic conductivities for five modeled aquifer layers.

Table 4.2 Final parameter values from model calibration.

Parameter types		Final parameter values: Mean	Median	Min	Max	Previous studies
Horizontal hydraulic conductivity (m/d)	Clay	6.81×10^{-3}	9.47×10^{-4}	1.92×10^{-6}	0.271	4.05×10^{-4}[1]
	BK	2.754	0.834	1.55×10^{-3}	73.261	1.9-98.2[1]
	PD	3.289	0.666	6.14×10^{-4}	100.0	1.7-183.6[1]
	NL	2.816	0.222	1.93×10^{-4}	100.0	1.8.-147.4[1]
	NB	8.889	0.315	1.64×10^{-4}	100.0	1.8-141.6[1]
Vertical anisotropy	Clay	27.437				N/A
	BK	4.605				
	PD	1.441				
	NL	10.000				
	NB	3.081				
Specific storage (S_s, m^{-1})	Clay	N/A (parameter is not sensitive)				$S = 10^{-3}$ to 10^{-4}[2]
	BK	8.33×10^{-7}	8.47×10^{-7}	4.61×10^{-7}	1.39×10^{-6}	
	PD	8.30×10^{-7}	8.13×10^{-7}	5.21×10^{-7}	1.68×10^{-6}	
	NL	8.82×10^{-7}	8.59×10^{-7}	5.56×10^{-7}	1.30×10^{-6}	
	NB	8.47×10^{-7}	8.30×10^{-7}	4.10×10^{-7}	1.48×10^{-6}	
Specific yield (S_y)	Clay	5.22×10^{-2}	4.37×10^{-2}	2.18×10^{-3}	0.222	
	BK	5.34×10^{-2}	3.50×10^{-2}	2.16×10^{-3}	0.228	
	PD	N/A (parameter is not sensitive)				
	NL					
	NB					
Recharge (mm/yr)		29.345	3.919	0.628	365.242	~5-150 [3]
Max evapotranspiration (mm/yr)		3.067	2.919	1.369	6.799	~750-800[4]
Riverbed conductance factor (m/d)	Chao Phraya	1.500				N/A
	Tha Chin	13.177				
General-head conductance factor (m^2/d/m)	W	6.087				N/A
	N	0.159				
	E	0.112				

(1) JICA, 1995
(2) Phisut technology Co. Ltd, 2012
(3) Faculty of Engineering Chulalongkorn University, 2009
(4) Panya Consultant Co., Ltd, 2009

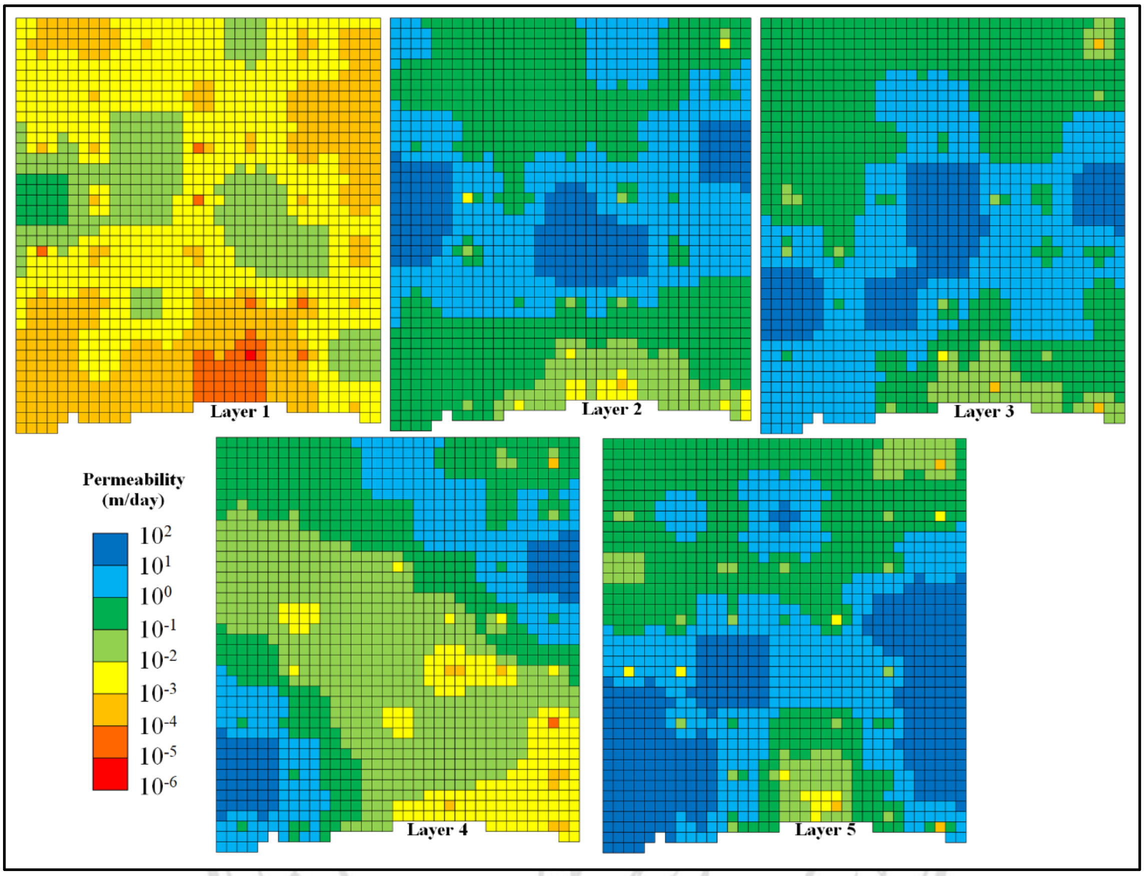

Figure 4.6 Distribution of hydraulic conductivities for five model layers after model calibration.

4.1.3 Sensitivity analysis of hydrologic parameters

Sensitivity analysis of the input parameters indicated how importance they affect the output values. In this study, the sensitivity analysis is proceeded with hydraulic conductivity, storativity (storage coefficient), GHB conductance, river-bed (RIV) conductance, recharge rate and maximum evapotranspiration rate. The sum of squared errors of hydraulic heads was used to evaluate relative sensitivities of model parameters. The calibrated input parameters are multiplied by 0.1, 0.3, 0.5, 0.8, 1, 3, 5, 8, and 10. Then the resulted sum of squared errors for each case was recorded and plotted as a function of multipliers. The results of sensitivity analysis are shown in Figure 4.7. The hydraulic conductivity, as expected, is the highest sensitive parameter where storage coefficient is the second most sensitive in this model. The other parameters' sensitivities are not significantly different.

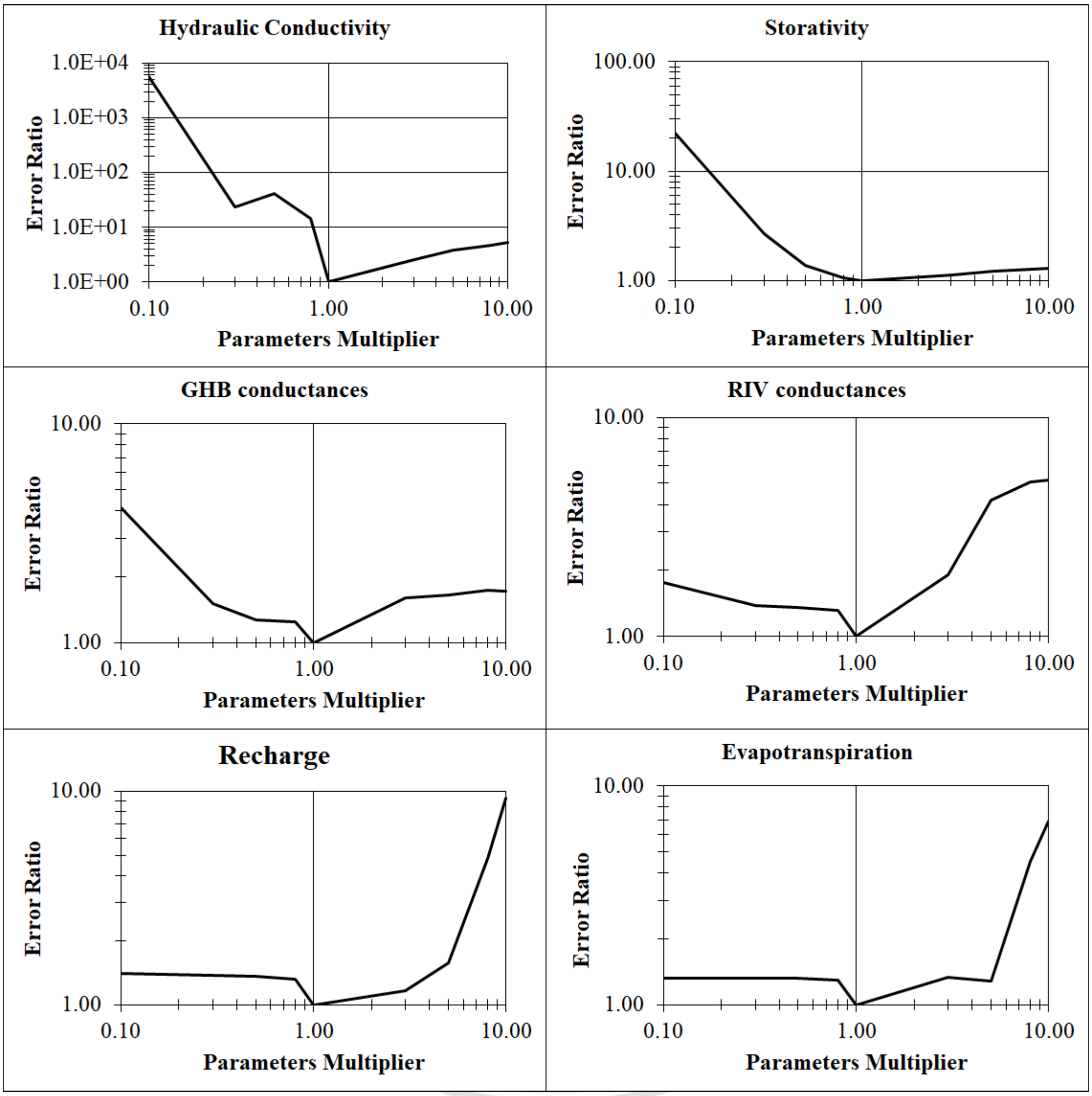

Figure 4.7 The relation between error ratio and parameters multiplier.

4.1.4 Future hydraulic head prediction

After transient model was successfully calibrated, the model was used to predict future hydraulic head distribution. As for example, the prediction of hydraulic head distribution in mostly utilized aquifer, the PD aquifer, is illustrated here. Projected (and, also, increasing) groundwater pumping rate scenario was used in the prediction. Hydraulic head distribution in PD aquifer (Layer 3) in January 2010 to January 2030 is shown in Figure 4.8. In 2010, there were 2 cones of depression: the larger one was in the northeastern part and the smaller one was in southwestern part but the smaller cone had lower groundwater level. The (partial) cones of depression become larger and deeper as time progresses in 2020 and 2030 as expected.

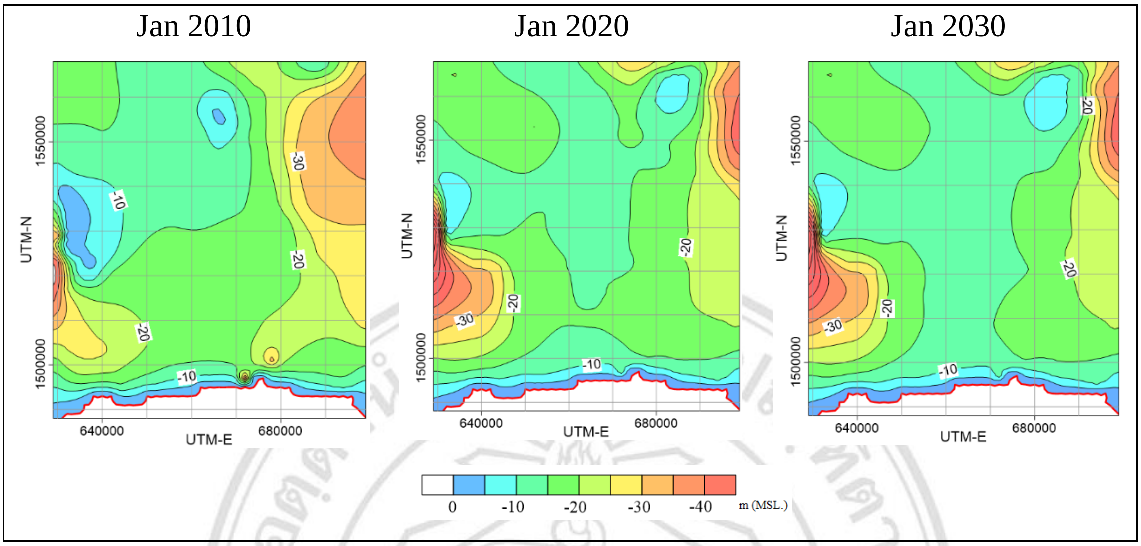

Figure 4.8 Example of predicted hydraulic head distribution in PD aquifer in 2020 and 2030.

4.2 Land subsidence simulation

Land subsidence was simulated using Interbed-Storage or IBS Package (Leake and Prudic, 1991) in MODFLOW program. The subsidence model utilized previously calibrated transient flow model with an activation of IBS package which requires skeleton component of elastic and inelastic storage coefficients. The model was manually calibrated using subsidence monitoring data from 37 locations. Example results of subsidence modeling and calibration are shown in Figure 4.9Figure 4.11. These plots illustrate time-varying calculated and observed subsidence. The positive value in vertical axis refers to land subsidence whereas negative value is surface rebound.

The model results can be divided into 3 groups based on a goodness of fit between modeled and observed data. Group 1 has the better fit among all observation points where values and trends for subsidence behavior can be modeled or captured. Group 2 is moderately well-fit whereas Group 3 are locations that model cannot fit the observed subsidence. The distribution of observation points of each group is shown in Figure 4.12. The observation points of Groups 1, 2, and 3 are mapped in green, blue, and red respectively. Group 1 (relatively good fit) distributes in the middle of Eastern part of model. Group 2, smaller number of points/locations, has random distribution whereas Group 3 is mostly distributed is near south boundary of model. The reason why Group 3 was unable to match the observation is because they are so close to the constant-head boundary in the southern part of the domain which affected both heads and subsidence simulation. Not only the boundary condition, but the goodness-of-fit of each group also depends on subsidence cause. Land subsidence in Group 1 is caused by groundwater extraction whereas land subsidence in Group 2 may be caused by other factors such as building loads and natural subsidence. Land subsidence in some locations, such as in Group 3, may be unrelated to groundwater level change. The best estimated skeleton component parameters form manual calibration model are 2.0×10^{-2} m^{-1} for elastic specific storage and 6.0×10^{-3} m^{-1} for inelastic specific storage.

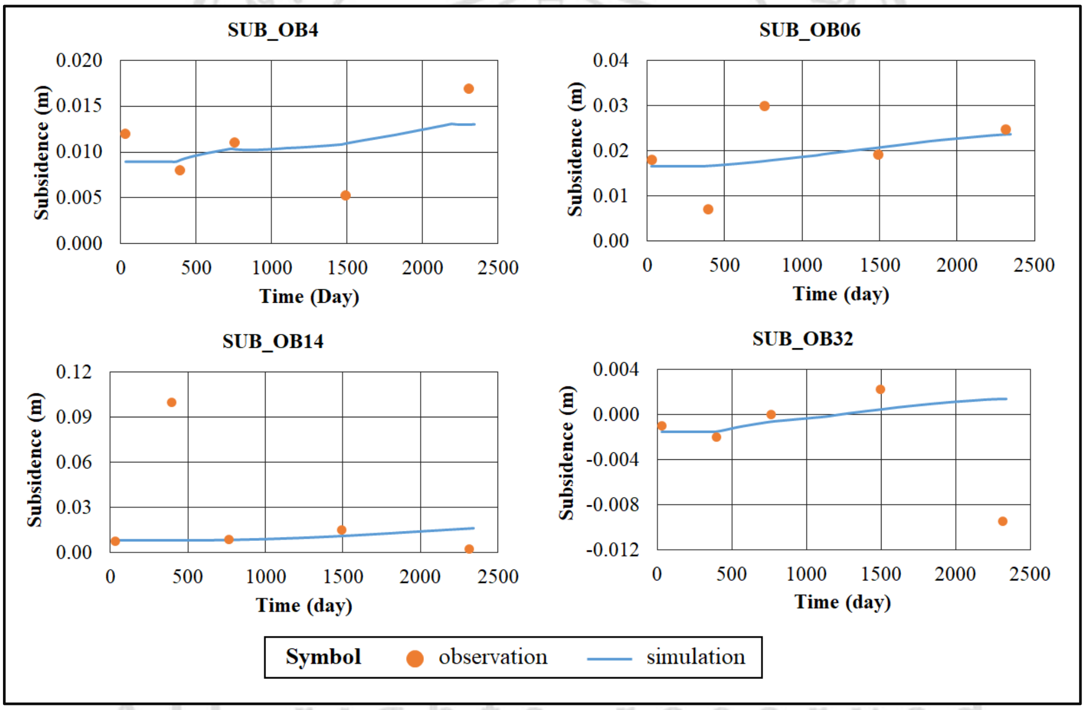

Figure 4.9 Examples of land subsidence simulation results (Group 1).

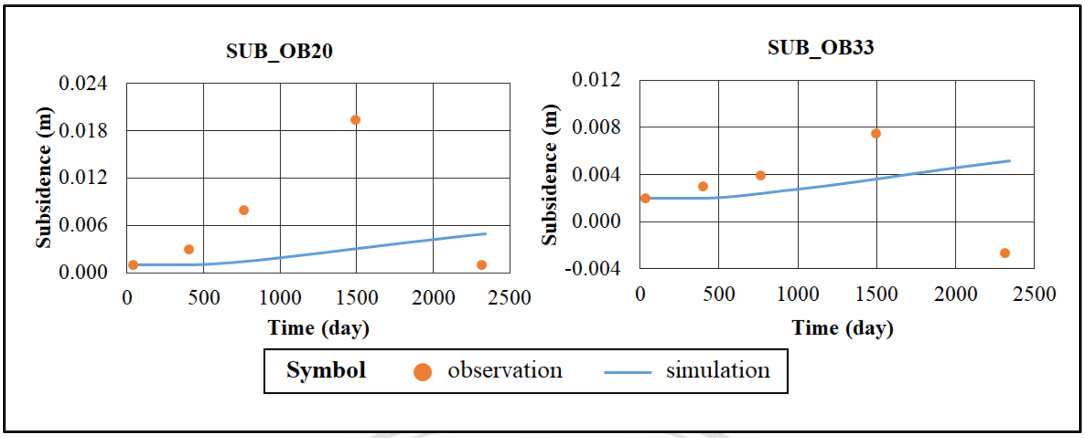

Figure 4.10 Examples of land subsidence simulation results (Group 2).

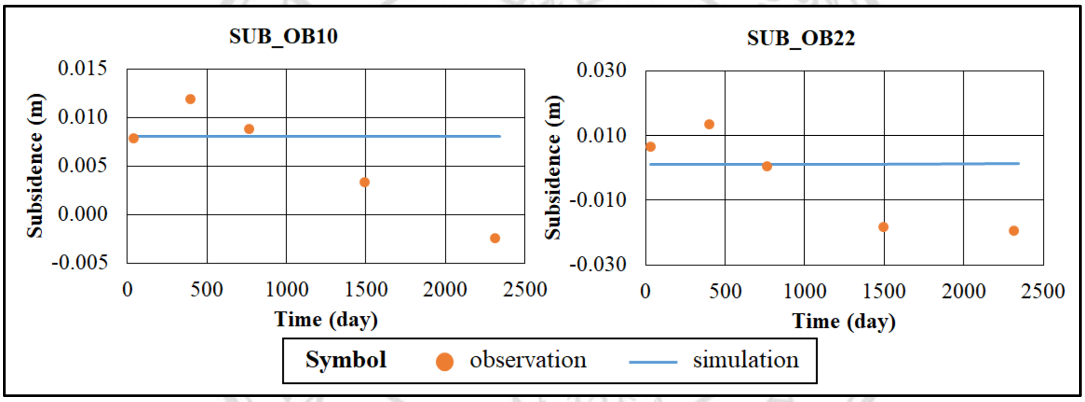

Figure 4.11 Examples of land subsidence simulation results (Group 3).

As mentioned earlier, the subsidence simulation in MODFLOW program is achieved through the use of IBS package. The IBS package uses groundwater level change and skeleton component parameters that are constant. In this study subsidence will be affected by only groundwater level change. The groundwater level is mainly controlled by groundwater extraction rate. The subsidence prediction is shown in Figure 4.13. If the pumping rate is high and groundwater level drops rapidly, subsidence will increase (Type 1). If pumping rate is relatively small and decrease or becomes stable, subsidence will be decrease or surface will rebound (Type 2). If pumping rate does not cause a lowering of groundwater level, surface elevation will be stabilized (Type 3). The maximum cumulative land subsidence from reliable points is about 6.5 cm at SUB_OB09 in Pathum Thani and maximum cumulative surface rebound is about 8 cm at SUB_OB37 in Bangkok.

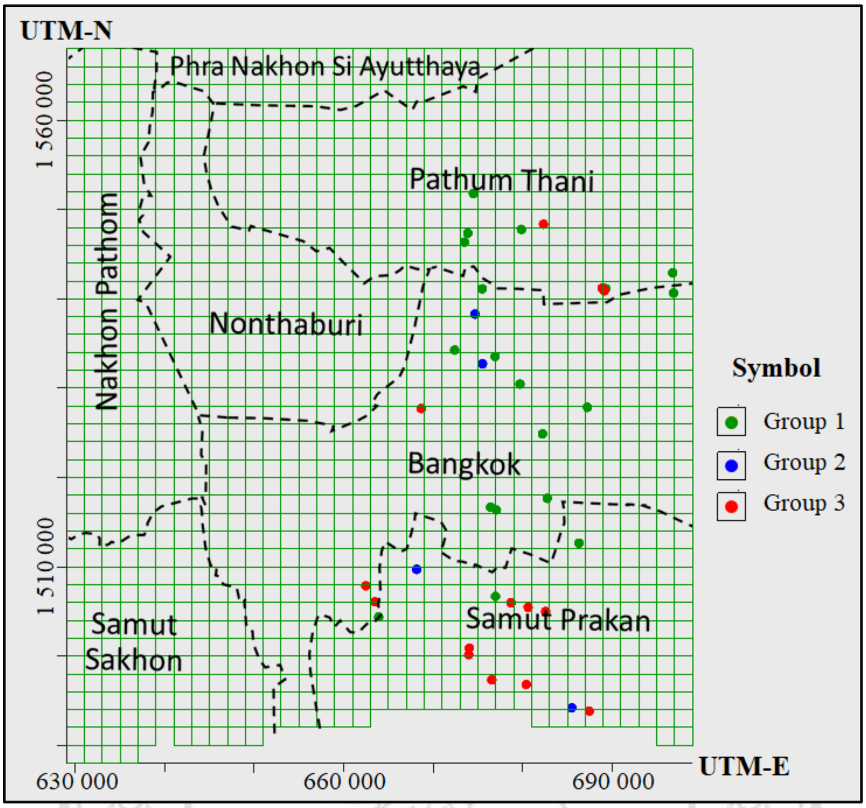

Figure 4.12 Location of observation points mapped by reliability.

4.3 Applications and limitation of the model

The results from steady-state groundwater flow model simulation suggested that groundwater extraction rate used in study area should be higher than the reported value. This finding corresponds to a study by Noipow et al. (2016) where they found actual (and unreported) groundwater usage based on Tritium and stable isotope study. Transient groundwater flow model simulation can match the 'trend' of historical hydraulic head in Bangkok aquifer system so the model cab be used to at least predict the groundwater level in groundwater management. The land subsidence model is able to capture the subsidence behavior in the eastern part of model whereas the western part still lacks of subsidence and head observation data. In the eastern part, the subsidence model captures subsidence behavior relatively well except in the south part of the study area the area is too close to the constant-head boundary condition. Subsidence in a few locations in Group 3 may be caused not only by groundwater level change but other factors such as loadings. Some locations show subsidence and subsequent rebound in prediction matches with recent observation (DGR, 2018). It is recommended that the actual groundwater usage should be acquired in order to obtain a more accurate and reliable simulations. The hydrologic parameters should also be evaluated from field investigation. The density-dependent model could be used in simulation because the south boundary of study area may have saltwater intrusion from the Gulf of Thailand. Current model grid of 2×2 km^2 could be refined to smaller grid system for accuracy improvement although the model execution and calibration time may takes longer. The land subsidence model should be calibrated automatically by PEST algorithm (Doherty 1994; Doherty, 2003) with pilot-point technique that may result in a better match with historical data. The groundwater and land subsidence prediction should be executed with several scenarios such as different future groundwater pumping rate. Other causes of land subsidence such as loading of building and land reclamation should also be considered.

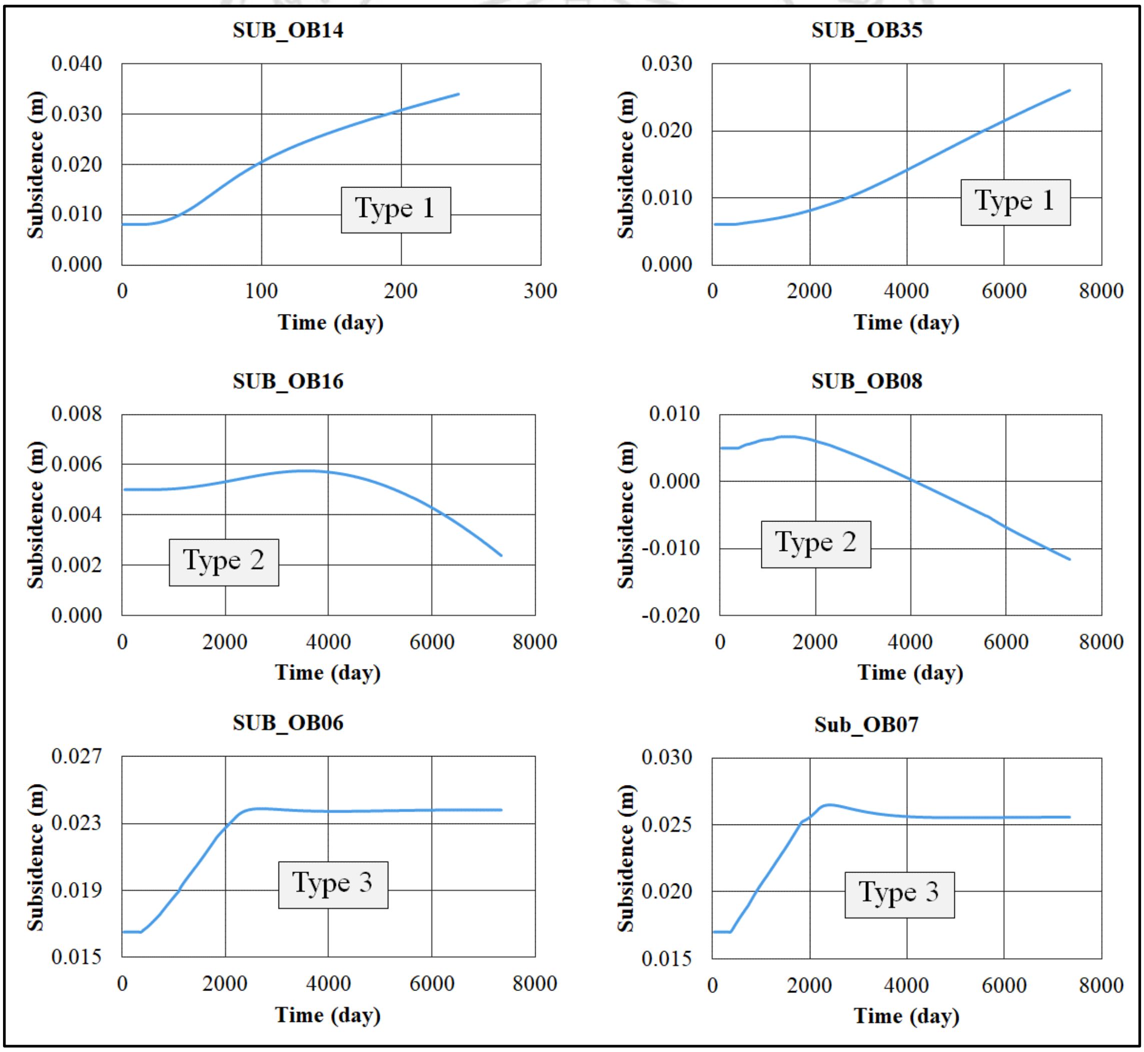

Figure 4.13 Land subsidence prediction simulation.

CHAPTER 5

CONCLUSIONS AND RECOMMENDATION

5.1 Conclusions

The groundwater flow and subsidence models of the Bangkok metropolitan area which includes Bangkok, Pathum Tani, Nakhonpathom, Samut Sakhon, Samut Prakan, and Phra Nakorn Si Ayutthaya were constructed based on previously documented data. The major aquifers of the Lower Chao Phraya aquifer system, which were simulated in this study consisted of five major materials: top clay layer, Bangkok (BK) aquifer, Phra Pradaeng (PD) aquifer, Nakhon Luang (NL) aquifer, and Nonthaburi (NB) aquifer. Other aquifers below the NB aquifer were disregarded because of the insignificant groundwater usage and they are separated by a thick and continuous clay layers. The 3-D finite-difference program, MODFLOW (Harbaugh *et al*., 2000; Harbaugh, 2005) was used to simulate aquifers' behavior with the simulated model domain of 70-km (E-W) wide, and 80-km (N-S) long. The study area was discretized into 35 columns, 40 rows, and 5 layers. There were 6,685 active cells of 2×2 km^2 uniform grid size but the layer thicknesses were varied. The flow model was simulated under both steady-state and transient conditions.

Model calibration is achieved using PEST (Doherty 1994; Doherty, 2003) with an application of a novel pilot-point technique where aquifer's heterogeneity can be simulated resulting in a greatly complex and highly parameterized model. The calibration targets were hydraulic heads obtained from 66 observation wells. The simulation period of January 2010 to June 2016 was divided into 77 stress periods with a period length of 1 month. The groundwater flow model calibration suggested that actual groundwater usage was 1.5 times higher than the reported value. The calibrated values (such as K, S, recharge, etc.) were in acceptable ranges with previous field investigations. Flow model can successfully capture large cone of depressions observed in the study area. The calibrated model was subsequently used to predict hydraulic head distribution until

January 2030. The predictive model based on projected groundwater usage showed that groundwater level, in most areas, tended to rise whereas the groundwater level in cones of depression became lowered. The northeast cone was smaller but the southwest cone was larger. There was a new cone of depression in the north. These cones are caused by high groundwater extraction rate.

After the flow model was successfully calibrated, it was used in the land subsidence simulation by activating the Inter-Bed Storage or IBS package. This model assumed land subsidence was mainly controlled by groundwater extraction rate. The model was further calibrated manually for the required parameters, elastic and inelastic storage coefficients, using the measured subsidence in 37 locations throughout the study areas. Because the flow model was successfully simulated, it was found that, by simply adding uniform elastic/inelastic coefficients in the IBS package, it could still capture subsidence behavior relatively well except for the southern part of the model where measurements was too close to the constant-head boundary (Gulf of Thailand). The land subsidence prediction was simulated until January 2030 and found that land subsidence tended to decrease in the most areas. The highest cumulative land subsidence was 6.5 cm in Pathum Thani and the highest surface rebound was found in Bangkok as 8.0 cm.

5.2 Recommendation

The sensitivity analysis of the flow/subsidence model found that most sensitive parameters of the model were hydraulic conductivities, storage coefficients. The reliability this modeling exercise could be increased by utilizing more measurements of hydraulic parameters and the actual groundwater extraction rates. Smaller model grid could definitely improve accuracy but simulation time will take much longer to execute. Adding additional aquifers below NB aquifer may not help obtain better results because no significant groundwater extractions existed. The use of density-dependent flow model may increase model's accuracy because of the possibility of the salt-water intrusion into the coastal aquifers at the south boundary. The subsidence model could be greatly improved with the use of pilot-point calibration technique which allows elastic/inelastic coefficients of the model aquifers to be heterogeneous, rather than uniform. Other causes of land subsidence such as building load and natural subsidence should also be taken into consideration.

REFERENCES

Anderson, M.P. and Woessner, W.W. 1992. Applied Groundwater Modeling—Simulation of Flow and Advective Transport. Academic Press, Inc., San Diego, CA, 381 p.

Anderson, M.P., Woessner, W.W., and Hunt, R. J. 2015. *Applied groundwater modeling: simulation of flow and advective transport (2nd edition)*. Academic press, Inc.

Asian Institute of Technology (AIT), 1981. Investigation of land subsid ence caused by deep well pumping in Bangkok area, Research Report, vol. 91. Asian Institute of Technology, Bangkok, Thailand.

Asian Institute of Technology (AIT), 1982. Groundwater Resources in Bangkok Area: Development and Management Study; Comprehensive Report 1978-1982. ATI Research Report no. 137 Submitted to the Office of the National Environment Board: Asian Institute of Technology, Bangkok, Thailand.

Barnett, B., Townley, L. R., Post, V., Evans, R. E., Hunt, R. J., Peeters, L., Richardson, S., Werner, A. D., Kanpton, A., and Boronkay, A., 2012. Australian groundwater modelling guidelines. National Water Commission, Canberra.

Chaithavee, S., 2015. INSAR Time Series Analysis for Land Subsidence Monitoring in Eastern Greater Bangkok, (Master degree's thesis) Faculty of Engineering, Chulalongkorn University, Bangkok, Thailand. (in Thai)

Faculty of Engineering Chulalongkorn University, 2009. The Analysis of Land Subsidence in Bangkok and its Vicinity Area project; Final Report Vol. 1/3: Main report Submitted to Department of Groundwater Resources: Faculty of Engineering, Chulalongkorn University, Bangkok, Thailand. (in Thai)

Cox, J.B., 1968. A Review of the Engineering Characteristics of the Recent Marine Clays in Southeast Asia, Research Report, vol. 6. Asian Institute of Technology, Bangkok, Thailand.

Darcy, H.P.G., 1856. *Les Fontaines publiques de la ville de Dijon. Exposition et application des principes à suivre et des formules à employer dans les questions de distribution d'eau, etc*. V. Paris: Delamont.

Department of Groundwater Resources (DGR), 2018, The study of effect in groundwater system in groundwater critical zone and lower Chao Phraya basin; The 3rd year progressing report. Retrieved 3 January 2019, Web site: http://gwlcp.nti.co.th (in Thai)

Doherty, J., 1994, PEST-Model-Independent Parameter Estimation. Watermark Computing, Corinda.

Doherty, J., 2003. Ground water model calibration using pilot points and regularization. *Groundwater*, *41*(2), 170-177.

Freeze, R.A. and Cherry, J.A., 1979. Groundwater: Englewood Cliffs. *New Jersey*.

Harbaugh, A.W., 2005, MODFLOW-2005, the U.S. Geological Survey modular ground-water model -- the Ground-Water Flow Process: U.S. Geological Survey Techniques and Methods 6-A16.

Harbaugh, A.W., Banta, E.R., Hill, M.C., and McDonald, M.G., 2000, MODFLOW-2000, the U.S. Geological Survey modular ground-water model -- User guide to modularization concepts and the Ground-Water Flow Process: U.S. Geological Survey Open-File Report 00-92, 121 p.

Heath, R.C. 1983. *Basic ground-water hydrology* (Vol. 2220). US Geological Survey.

Institute for Global Environment Strategies (IGES), 2007. Sustainable Groundwater Management in Asian cities, a final report of Research on Sustainable Water Management Policy, p. 25 to p. 43.

Japan International Cooperation Agency (JICA), 1995. The study on management of Groundwater and land subsidence in Bangkok metropolitan area and vicinity, Report submitted to Department of Mineral Resources and Public Works Department, Thailand, p.1-1 to p.11-5.

Jarvis A., H.I. Reuter, A. Nelson, and E. Guevara., 2008, Hole-filled seamless SRTM data V4, International Centre for Tropical Agriculture (CIAT), Retrieved 25 May 2017 Web site: http://srtm.csi.cgiar.org.

Konikow, L.F., Hornberger, G.Z., Halford, K.J., and Hanson, R.T., 2009, Revised multi-node well (MNW2) package for MODFLOW ground-water flow model: U.S. Geological Survey Techniques and Methods 6–A30, 67 p.

Leake, S.A., and Prudic, D.E., 1991. *Documentation of a computer program to simulate aquifer-system compaction using the modular finite-difference ground-water flow model* (pp. 06-A2). US Department of the Interior, US Geological Survey.

Likitlersuang, S., Teachavorasinskun, s., Surarak, C., Oh, E., and Balasubramanian, A., 2013. Small strain stiffness and stiffness degradation curve of Bangkok Clays. Soil and Foundation, 53(4), 498-509.

McDonald, M.G., and Harbaugh, A.W., 1988, A modular three-dimensional finite-difference ground-water flow model: U.S. Geological Survey Techniques of Water-Resources Investigations, book 6, chap. A1, 586 p.

National Statistical Office (NSO), 2016, Statistics of Rainfall at Meteorology Station in a period of 2003-2015. Retrieved 21 May 2017, Web site: http://service.nso.go.th

Nguyen, A.D., 1999. Updating and Analysis of Bangkok Land Subsidence Caused by Deep Well Pumping with Emphasis on Shallow Soil Settlement. A Master of Engineering degree Thesis No. GE-28-1, Asian Institute of Technology, Bangkok, Thailand.

Nutalaya, P., and Rau, J.L., 1987. Structural framework of the Chao Phraya basin, Thailand. Proceedings of Symposium on Cenozoic Basin Thailand: Geology and resources, Bangkok, Thailand, p. 106 to p.129.

Nutalaya, P., Yong, R.N., Chumnankit, T., and Buapeng, S., 1989. Land subsidence in Bangkok during 1978-1988. Proceedings of Workshop on Bangkok Land Subsidence-What is Next? Bangkok, June, p. 1 to p.48.

Panya Consultant Co., Ltd, 2009. Evaluate groundwater potential by using mathematical model to find safe yield for each providence in Tha Chin and Mae Klong river basin project. Final Report Submitted to Department of Groundwater Resources: Bangkok, Thailand. (in Thai)

Phien-wej N., Giao, P.H., and Nutalaya, P., 2006. Land subsidence in Bangkok, Thailand. Engineering Geology, 82, 187-201.

Phisut technology Co., Ltd, 2012. The systematically survey and study of land subsidence in in groundwater critical zone, Final Report Submitted to Department of Groundwater Resources: Bangkok, Thailand. (in Thai)

Pianchareon, C., 1976. Groundwater and land subsidence in Bangkok, Thailand Proceedings of Second International Symposium on Land Subsidence, Anaheim, California, pp. 355-364.

Ramnarong V., Buapeng, S., Chootnatut, S., and Loupensri, A., 1998. Groundwater and land subsidence crisis in Bangkok metropolitan and vicinity. Technical report, vol. 3/1998. Department of Mineral Resources, Bangkok, Thailand.

Rotchanameka, S., and Mairaing, W., 2013. The Characteristic of Aquifer Drawdown and Settlement of Bangkok and Vicinity Area. Electronic Journal of Geotechnical Engineering (EJGE), vol. 18 (2013) Bund. W, 5573-5583.

Shah, N., Nachabe, M. and Ross, M., 2007. Extinction depth and evapotranspiration from ground water under selected land covers. *Groundwater*, *45*(3), pp.329-338.

Terzaghi, K., 1943, Theoretical Soil Mechanics, John Wiley and Sons, New York, 510p.

Todd, D. K., & Mays, L. W. (1980). Groundwater hydrology. John Willey Sons. *Inc.*, *New York*, *535*.

CURRICULUM VITAE

Author's Name Mr. Pee Poatprommanee

Date/Year of Birth 21 Much 1993

Place of Birth Phrae Province, Thailand

Education 2005-2011 Nareerat School Phrae

2011-2014 Bachelor of Science in Geology (First class honors, silver medal), Chiang Mai University

Scholarship Science Achievement Scholarship of Thailand (SAST)

Publication Poatprommanee, P., Seanton, S., 2018. Groundwater flow model of Bangkok and vicinity area. 7th International Symposium on the Fusion of Science & Technologies (ISFT 2018). 16th-20th December 2018. Bangkok, Thailand.